Base pair opening in a damped helicoidal Joyeux-Buyukdagli model of DNA in an external force field

J. B. Okaly,[1,2,*] A. Mvogo,[1,2,†] C. B. Tabi,[3,‡] H. P. Ekobena Fouda,[1,§] and T. C. Kofané[1,2,‖]

[1]*Department of Physics, Faculty of Science, University of Yaounde I, P.O. Box 812, Yaounde, Cameroon*

[2]*African Centre of Excellence in Information and Communication Technologies, University of Yaounde I, P.O. Box 8390, Yaounde, Cameroon*

[3]*Botswana International University of Science and Technology, Private Bag 16 Palapye, Botswana*

(Received 9 June 2020; accepted 21 October 2020; published 1 December 2020)

Upon the Joyeux-Buyukdagli model of DNA, the helicoidal interactions are introduced, and their effects on the dynamical behaviors of the molecule investigated. A theoretical framework for the analysis is presented in an external force field, taking into account Stokes and hydrodynamics viscous forces. In the semi-discrete approximation, the dynamics of the molecule is found governed by the cubic complex Ginzburg-Landau (CGL) equation. By choosing an appropriate decoupling ansatz, the cubic CGL equation is transformed into a nonlinear differential equation whose analytical solitary wave-like solutions can be explored by means of the direct method, which is more tractable in case where the form of soliton solutions is known. Based on this, a dissipative bright-like soliton solution is obtained. Numerical experiments have been done, and relevant results were brought out, such as the quantitative and qualitative influences of the helical interactions on the parameters of the traveling bubble. The important role-played by these interactions in the DNA biological processes is brought out, showing that depending on the wave number, their effects can increase, decrease, or keep constant the bubble angular frequency, velocity, amplitude, and width, as well as the energy involved by enzymes in the initiation of DNA biological processes. This can prevent some coding or reading errors and resulting genetic damages. Analytical predictions and numerical experiments were in good agreement.

DOI: 10.1103/PhysRevE.102.062402

I. INTRODUCTION

In the last decades, a great deal of attention has been given to nonlinear discrete systems [1–4] as a consequence of the diversity of many applications to physical and biological phenomena [5,6]. For example, the understanding of the nonlinear dynamics of deoxyribonucleic acid (DNA), which is one of the most fascinating problems of modern biophysics because, in relation to its functions, DNA stores and protects all information that living organism needs to grow and reproduce. Since the discovery of its double helix structure [7], DNA has been the subject of various studies containing complex and important knowledge. The dynamics of DNA provides various biological processes such as, replication, transcription, translation, and transmission of genetic codes, just to mention a few.

More recently, it has been shown that external agents (or inhomogeneities) present in DNA molecular environment can attack the molecule in an open state configuration, during which the code has to be read. These attacks modified the parameters of the open state, what can create reading or coding errors, which can cause unfavorable genetic mutations responsible for an estimated 6000 diseases, including all cancers [8–10]. Known as replicative senescence, the humans cells are naturally programed to divide approximatively 50 times, to continuously replace defective or dead cells, what extend our lifespan [11]. It has been also shown that genetic mutations, which are not inherited in the vast majority, but occur over the course of our lifetime can be eliminated, every DNA cell will replace itself perfectly during cell division, and the humans lifespan will achieve approximately 120 years [12]. Along the same line, it was found that the number of DNA attacks in a single humans cell exceeds 10 000 every day [13]. Since the nature selects generally DNA molecules in a noisy crowded environment, it is very important to block genetic mutations during our lifetime.

Among the most powerful mutation-blocking agents is *chlorophyllin*, which is a semi-synthetic, water-soluble form of the plant pigment *chlorophyll*. It possesses DNA damage-protection and DNA repair processes effects at much lower amounts [14,15]. The *Chlorophyllin* actions limit the production of molecular structures formed when an external agent bonds with DNA. They decrease the harmful activities of some enzymes, which attack the DNA molecule, and present biochemical errors of varying degrees of severity [8,16]. It seems that all these DNA repair processes caused by the actions of *chlorophyllin* can modify some DNA molecular parameters, such as the long-range interactions (LRI) [17,18], hydrogen bonds angle [19], transport memory effects [20], or stacking or helicoidal interactions [21–24].

Moreover, the spatial structure of the DNA molecule implies the helicity of the double strands model. Although this helicity is obvious, some authors demonstrated that when helical interactions were considered, the wave switching was possible [21], while others showed that increasing the helical interactions destroys the soliton profile with time [22]. By the way, Daniel and Vasumathi [23], and then Tabi *et al.* [25],

*Corresponding author: okalyjoseph@yahoo.fr
†mvogal_2009@yahoo.fr
‡tabic@biust.ac.bw
§hekobena@gmail.com
‖tckofane@yahoo.com

also indicated that the increasing of the helical interactions provides a better representation of the bubble traveling in the DNA molecule by involving a larger number of base pairs in the bubbles. Indeed, according to the later, the helical interactions introduce a lengthscale variation in the bubble width, while its profile is not affected. Thus, the effects of helicity on DNA base pairs opening is far from been understood.

The key problem in this work is to investigate on the impact of the helicoidal interactions on the dynamical properties of the DNA molecule to know their contributions in the DNA repair processes and how the genetic code is protected. For this purpose, we add helical interactions to the original model of DNA by Joyeux-Buyukdagli (JB) [26], instead of the spin-like model used in Refs. [21–23]. We focus on the angular frequency, group velocity, amplitude, and width of the soliton solution, when the helicoidal interactions evolve. To attempt this issue, we consider the homogeneous DNA molecule in a damped medium by taking into account an external force field. A detailed study of the equation of motion is done in the semi-discrete approximation and a cubic complex Ginzburg-Landau (CGL) equation found.

A breather-like soliton solution representing an open state configuration in an individual strand of DNA, which collectively represents a bubble moving in the DNA chain, is obtained. Also found in numerous works, the soliton was obtained in the DNA dynamics for the first time, as a result of simulations of one strand of the molecule. The other strand was used as a source of an interacting gravitational potential field [27], analog of the gravitational field in the mechanical model of Scott [28].

The rest of the paper is structured as follows. Section II is devoted to the presentation of the model Hamiltonian and discrete equations of motion for the in-phase and out-of-phase motions, respectively. Using the multiple scale expansion method in the semi-discrete approximation, the nonlinear dynamics of the molecule is presented in the nonviscous and nonforced limit. In Sec. III, in a weakly external forces field, the molecule is considered in the heavily damped medium by taking into account the Stokes and hydrodynamics viscous forces. Through the semi-discrete approximation together with the direct method that has been used with success in the nonlinear Schrödinger (NLS) equation with dissipation by Kengne *et al.* [29], the bright-like soliton solution of the equation of motion for the out-of-phase motion is derived. Numerically and analytically, the qualitative and quantitative impacts of the helical interactions on the dynamics of the DNA molecule are discussed in the same section. The comparison between numerical simulations of the soliton propagates in the viscous and nonviscous medium is also done. Finally, a brief summary of the paper is given in Sec. IV.

II. MODEL HAMILTONIAN AND EQUATION OF MOTION

In this work, we strongly rely on the extended model for DNA dynamics, first introduced by Joyeux and Buyukdagli [26]. Since the work of Watson and Crick [7], the DNA molecule is known to be twisted. Thus, the double helix makes the molecule helicoidal. By considering the helicoidal geometry of the chain, the bases which, although distant along the double helix become close in three-dimensional space [30]. Thus, one observes the appearance of new interactions mediated by water filament and which bridge the nonadjacent bases in a sequence. Such interactions yield qualitative and quantitative changes in the dynamical behaviors of the model [30–32]. In fact, indirect experiments and results from Monte Carlo simulations indicate that water filaments make it possible for phosphate groups from opposite major grooves to interact [34,35]. This otherwise means that a nucleotide at the site nth of one strand interacts with both $(n+h)$th and $(n-h)$th nucleotides of the other strand. Since the DNA helicoidal pitch is about 10 base pairs per turn, it is suitable to assume $h = 5$.

Moreover, the topological constraints such as activation or repression effects usually observed during the conformational changes are induced by the helicoidal interactions. Indeed, during DNA processes related to opening of base pairs, a local unwinding of the helix with a local extra twist at the two ends of the bubble is observed. This unwinding, which is due to the topological constraints causes a long-range elastic stress [33]. It is well known that the bases are hydrophobic. Thus, the helicoidal structure of the DNA chain can be also seen as a natural protection for bases from solvating water. Therefore, the helicoidal interactions play a crucial in DNA molecule, they contribute to protect the genetic code.

In the following, the helicoidal interactions are restricted to the forces that appear due to the proximity is space of bases of opposite strands. Therefore, to the original JB DNA model, helical interactions are added in the sense of Dauxois [36]. The resulting helicoidal JB model of DNA consider DNA molecule as two elastic chains of nucleotides, which represent both strands of the molecule. In the same strand, the nucleotides are linked by the nearest-neighbor interactions along the chains, and connected to each of the other strand by the hydrogen bonds. The molecule is assumed homogeneous and twisted, only transverse motions of DNA base pairs are taken into consideration, while the longitudinal, rotation, and torsional motions are neglected. Therefore, the model includes two degrees of freedom. The parameter n defines a position of the nucleotide pair, while x_n and y_n are the transverse displacements from the equilibrium position of nucleotides located on opposite strands. The Hamiltonian of such a model is written as

$$H = \sum_n \left\{ \frac{1}{2} m\left(\dot{x}_n^2 + \dot{y}_n^2\right) + U_n(x_n, y_{n-h}, y_{n+h}) + V_n(x_n, y_n) + W_n(x_n, y_n, x_{n-1}, y_{n-1}) \right\}, \quad (1)$$

where

$$U_n(x_n, y_{n-h}, y_{n+h}) = \frac{1}{2} k[(x_n - y_{n-h})^2 + (x_n - y_{n+h})^2],$$

$$V_n(x_n, y_n) = D_0[e^{-a(x_n - y_n)} - 1]^2,$$

$$W_n(x_n, y_n, x_{n-1}, y_{n-1}) = \frac{\Delta H_n}{C}\left[2 - e^{-b(x_n - x_{n-1})^2} - e^{-b(y_n - y_{n-1})^2}\right] + K_b[(x_n - x_{n-1})^2 + (y_n - y_{n-1})^2],$$

where m is the average mass of the nucleotides independent of the precise nature of the base pair at position n, and N represents the number of the base pairs of the chain. The function U_n describes helical interactions. That is, a harmonic coupling energy that connect a nucleotide nth of one strand to both the $(n+h)$th and $(n-h)$th nucleotides on the other strand. The on-site potential $V_n(x_n, y_n)$ is due to the presence of hydrogen bonds in base pairs. In the Peyrard-Bishop model, such interactions are described by the Morse potential of depth D_0 (also known as the dissociation energy) and width a. The Morse potential is an increasing function of the distance between the two bases of a pair n, and therefore opposes the breaking of the hydrogen bonds. The potential W_n is the sum of the two terms, namely, the backbone stiffness and the stacking potential. Both terms are increasing functions of $|x_n - x_{n-1}|$ (as well as $|y_n - y_{n-1}|$), they oppose the stacking (separation of successive bases belonging to the same strand) of the bases. This stacking potential is modelled by a Gaussian hole of depth $\frac{\Delta H_n}{C}$. It results essentially from hydrophobic interactions with the solvent, and electronic interactions between successive base pairs on the same strand. At last, the backbone stiffness is taken as a harmonic potential of constant K_b. Its role consists in preventing dislocation of the strands, by ensuring that base pairs belonging to the same strand do not separate infinitely when approaching the melting temperature.

The above three functions, namely, U_n, V_n, and W_n, should depend on the type of base pair. However, in the model under study, the DNA molecule is assumed to be homogeneous. Thus, all the above parameters keep their numerical values along the DNA chain. All the nucleotides are assumed to be discs with the same mass, therefore the value of the nucleotide mass mentioned above is the average of the four possible values.

The values of parameters used to perform our analysis are those from the dynamical and denaturation properties of DNA. They are [26] $m = 300$ amu, $D_0 = 0.04$ eV, $a = 4.45$ Å^{-1}, $\Delta H = 0.44$ eV, $b = 0.10$ Å^{-2}, $K_b = 10^{-5}$ eVÅ^{-2}, and $\frac{\Delta H}{C} = 0.22$ eV. In this system of units (amu, Å, eV), a new time unit (tu) is defined as $1\text{tu} = 1.018\times10^{-14}$ [37].

It is convenient to introduce the coordinates u_n describing the movement of a center of mass of the nucleotide pair, and v_n a stretching of the nucleotides belonging to the same pair defined as

$$u_n = \frac{x_n + y_n}{\sqrt{2}}, \quad \text{and} \quad v_n = \frac{x_n - y_n}{\sqrt{2}}, \tag{2}$$

where u_n and v_n represent the in-phase and out-of-phase motion, respectively. That is, the sum and difference displacements of the bottom and top strands, respectively. Based on the above, Eq. (1) becomes

$$H = \sum_n \left\{ \frac{1}{2} m \dot{u}_n^2 + U(u_n) + W(u_n) \right\} + \sum_n \left\{ \frac{1}{2} m \dot{v}_n^2 + U(v_n) + V(v_n) + W(v_n) \right\}, \tag{3}$$

where

$$\begin{aligned} U(u_n) &= \frac{1}{2} k[(u_n - u_{n-h})^2 + (u_n - u_{n+h})^2], \\ U(v_n) &= \frac{1}{2} k[(v_n + v_{n-h})^2 + (v_n + v_{n+h})^2], \\ V(v_n) &= D_0[e^{-a\sqrt{2}v_n} - 1]^2, \\ W(u_n) &= \frac{\Delta H_n}{C}\left(1 - e^{-b(u_n - u_{n-1})^2}\right) + K_b(u_n - u_{n-1})^2, \\ W(v_n) &= \frac{\Delta H_n}{C}\left(1 - e^{-b(v_n - v_{n-1})^2}\right) + K_b(v_n - v_{n-1})^2. \end{aligned} \tag{4}$$

From the Hamiltonian given in Eq. (1), it is possible to obtain two nonlinear partial differential equations describing the in-phase and out-of-phase motions of the DNA molecular chain, respectively. This leads to

$$\begin{aligned} \ddot{u}_n = {} & \frac{2K_b}{m}[(u_{n+1} - u_n) + (u_{n-1} - u_n)] \\ & + \frac{k}{m}[(u_{n+h} - u_n) + (u_{n-h} - u_n)] \\ & + \frac{2b\Delta H_n}{mC}\big[(u_{n+1} - u_n)e^{-b(u_{n+1} - y_n)^2} \\ & \qquad + (u_{n-1} - u_n)e^{-b(u_{n-1} - u_n)^2}\big], \end{aligned} \tag{5a}$$

$$\begin{aligned} \ddot{v}_n = {} & \frac{2K_b}{m}[(v_{n+1} - v_n) + (v_{n-1} - v_n)] \\ & - \frac{k}{m}[(v_{n+h} + v_n) + (v_{n-h} + v_n)] \\ & + \frac{2b\Delta H_n}{mC}\big[(v_{n+1} - v_n)e^{-b(v_{n+1} - v_n)^2} \\ & \qquad - (v_{n-1} - v_n)e^{-b(v_{n-1} - v_n)^2}\big] \\ & + \frac{2\sqrt{2}aD_0}{m} e^{-a\sqrt{2}v_n}[e^{-a\sqrt{2}v_n} - 1]. \end{aligned} \tag{5b}$$

In what follows, it is assumed that the oscillations of bases are large enough to be anharmonic, but still insufficient to break the bond since the plateau of the Morse potential is not reached. Therefore, the base nucleotides are presumed to oscillate around the bottom of the Morse potential. We obtain, up to the third order of the Taylor expansion of exponential functions, the following equation of motion:

$$\begin{aligned} \ddot{u}_n = {} & J[(u_{n+1} - u_n) + (u_{n-1} - u_n)] \\ & + K[(u_{n+h} - u_n) + (u_{n-h} - u_n)] \\ & - S[(u_{n+1} - u_n)^3 + (u_{n-1} - u_n)^3], \end{aligned} \tag{6a}$$

$$\begin{aligned} \ddot{v}_n = {} & J[(v_{n+1} - v_n) + (v_{n-1} - v_n)] \\ & - K[(v_{n+h} + v_n) + (v_{n-h} + v_n)] \\ & - S[(v_{n+1} - v_n)^3 + (v_{n-1} - v_n)^3] \\ & - \omega_g^2\left(v_n + \alpha v_n^2 + \beta v_n^3\right), \end{aligned} \tag{6b}$$

where $J = [\frac{2K_b}{m} + \frac{2b\Delta H_n}{mC}]$, $S = \frac{2b^2\Delta H_n}{mC}$, $K = \frac{k}{m}$, $\omega_g^2 = \frac{4a^2D_0}{m}$, $\alpha = -\frac{3a}{\sqrt{2}}$, and $\beta = \frac{7a^2}{3}$.

By comparing Eqs. (6a) and (6b), one observes that the nonlinear effects are more important in Eq. (6b). The ad-

ditional nonlinear terms in Eq. (6b) come from the Morse potential, which models the hydrogen bonds interactions. Present in all biological systems, the hydrogen bonds are weak bonds, which induce nonlinear effects.

It is well known that the out-of-phase motion is supported by the weak hydrogen bonds, it describes the pair stretching, while the in-phase motion is related to the strong covalent forces. Thence, the contribution of the amplitude of in-phase oscillations in the DNA dynamics is little enough or sometimes insistent. In the best of the cases, the in-phase oscillations are detected as noise [38]. Therefore, the dynamics of the DNA molecule can be well described by Eq. (6b). For this reason, in what follows, our investigations will be limited to the analysis of the stretching motion of each base pair represented by the soliton solution of Eq. (6b).

To solve this equation, the multiple scale expansion method appears as the appropriate mathematical technique because in the DNA molecule, the stacking interactions between adjacent base pairs are weak [37,39]. As mentioned above, the small amplitude oscillation is assumed and the soliton solution setting in the form

$$\begin{aligned} v_n =& \varepsilon(F_{n,1}e^{i\theta_n} + F^*_{n,1}e^{-i\theta_n}) \\ &+ \varepsilon^2[F_{n,0} + (F_{n,2}e^{2i\theta_n} + F^*_{n,2}e^{-2i\theta_n})], \end{aligned} \tag{7}$$

where $\varepsilon \ll 1$ is n arbitrary small real number, and $\theta = qrn - \omega t$ the phase of the soliton. The parameters q and ω being the wave number and the optical frequency of the linear approximation of the base pairs vibrations. The notation * stands for complex conjugate. Therefore, after some algebra, one can express the functions F_0 and F_2 as [20]

$$F_0 = \mu|F_1|^2, \quad F_2 = bF_1^2, \tag{8}$$

where F_1 is the solution of the following standard NLS equation, with rescaled variable $x = \varepsilon(z - v_g t)$ with $\tau = \varepsilon^2 t$:

$$i\frac{\partial F_1}{\partial \tau} + P\frac{\partial^2 F_1}{\partial x^2} + Q|F_1|^2F_1 = 0, \tag{9}$$

where

$$\begin{aligned} P =& \frac{1}{2\omega}\left\{r^2[J\cos(qr) - Kh^2\cos(qrh)] - v_g^2\right\}, \\ Q =& -\frac{\omega_g^2\alpha}{\omega}\left[\mu + \frac{3}{2}\beta/\alpha + BC\right] + \frac{6S}{\omega}[1-\cos(qr)]^2, \end{aligned} \tag{10}$$

with

$$\begin{aligned} B =& 4\omega^2 - \varsigma, \quad C = \frac{\omega_g^2\alpha}{B^2 + D^2}, \quad D = 0, \\ \varsigma =& \omega_g^2 + 4J\sin^2(qr) + 4K\cos^2(qrh), \\ \mu =& -2\alpha\left[1 + \frac{4K}{\omega_g^2}\right]^{-1}, \quad b = BC + iDC. \end{aligned} \tag{11}$$

The angular frequency and group velocity are given by

$$\begin{aligned} \omega^2 =& \omega_g^2 + 4J\sin^2(qr/2) + 4K\cos^2(qrh/2), \\ v_g =& \frac{r}{\omega}[J\sin(qr) - Kh\sin(qrh)]. \end{aligned} \tag{12}$$

Equatin (9) is the CGL equation, its regulates the dynamics of the envelope soliton in the DNA molecular chain. The real parameters P and Q are the dispersion and nonlinearity coefficients, respectively.

For small wave number $q \ll 1$, the large-width soliton is observed [36]. Indeed, from Eq. (12) it is noticable that for the large soliton, which corresponds to small wave number, the group velocity, and the angular frequency of the soliton are positive if and only if $K < \frac{J}{h^2}$. This corresponds to the threshold maximal value of the helicoidal interaction constant $K_{\max} = \frac{J}{h^2}$. That is, for the values of K smaller than the threshold maximal value, a vibration moving in the positive x can be developed in the DNA molecular chain. Meanwhile, a localized soliton can be observed in the DNA molecule only if the helical interactions constant is less than the stacking constant $K < \frac{J}{h^2}$ [23,40]. These results are in good agreement with experimental observations [41–43].

We set $h = 5$ because the helix has a pitch of about ten nucleotide pairs per turn [44]. Thus, in the framework of the helicoidal JB DNA model studied in the present work, the threshold maximal value of the helicoidal interactions constant is $K_{\max} = \frac{J}{25} = 5.87.10^{-6}$ eV Å^{-2}. Meanwhile, the distance between nearest neighbors in the intrastrand coupling is smaller than the distance between nearest neighbors in the helical coupling. Although both energies are naturally similar, the helical coupling energy is less important than intrastrand coupling energy.

Its well known that the sign of the product PQ determines the type of the soliton solution of the NLS equation [45]. For instance, when $PQ < 0$, the plane wave solution is stable, and the system has a dark-type soliton solution also known as envelope hole. It is a finite-amplitude plane wave with a dip near $x = x_0$, such a solution does not correspond to the small amplitude limit of breather mode. The case $PQ > 0$ corresponds to unstable plane waves solution, which tends to split into wave packets that evolve into localized envelope soliton-like excitations of a bell shape, with a vanishing amplitude at $|x| \to \infty$. Accordingly, the breathing mode is observed in the DNA molecule. In the following, we restrict ourselves to small wave number ($q \ll 1$) selected in the range of $PQ > 0$, for which the localized soliton solutions of a bell shape with a large width is observed.

In Fig. 1, in the nonviscous and nonforced medium, we present the angular frequency ω, group velocity v_g, and the product PQ, of the soliton in terms of wave number q, as a function of the helicoidal interactions constant. The lines clearly show that the angular frequency which is an increasing function of both wave number and helicoidal interactions parameter K [see Fig. 1(a)], while the other parameters decrease, increase, or remain constant when the helicoidal interactions strength changes. For example, while the angular frequency of the soliton always increases with both wave number and helicoidal interaction constant, the group velocity decreases if $0 < q < 0.185$, and increases for $0.185 < q$. The cases $q = 0$ ($v_g = 0$, stationary wave) and $q = 0.185$ correspond to situations for which the group velocity is complectly independent on the helicoidal interactions [see Figs. 1(b) and 1(d)]. Moreover, we found out that for $\sigma = \sigma_+$, the product PQ (see Fig. 3) and the group velocity are positive if an only if the wave number is selected in a finite interval,

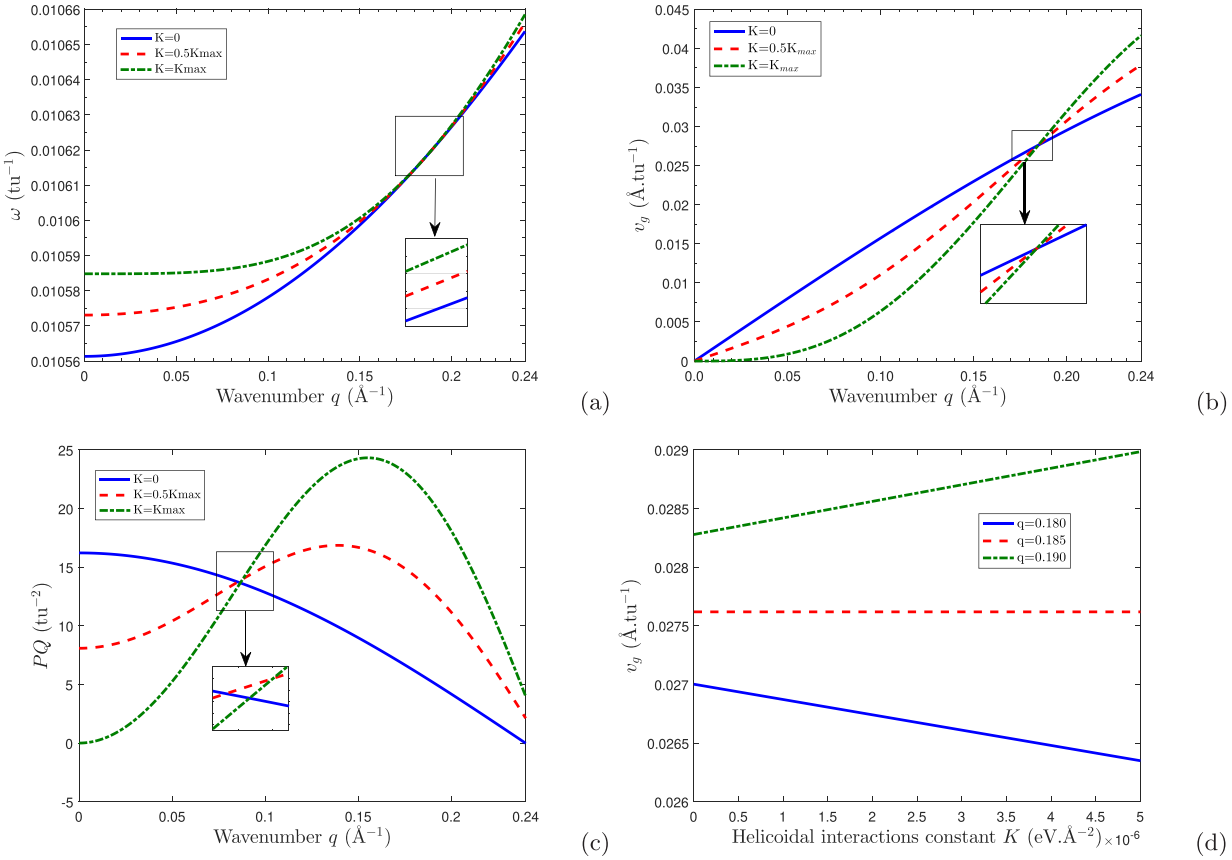

FIG. 1. Panels (a), (b), and (c) present the angular frequency, the group velocity, and the product PQ of the wave in the nonviscous and nonforced medium in terms of the wave number q, for different values of the helicoidal interactions constant, respectively. Panel (d) represents the evolution of the group velocity in terms of helicoidal interactions parameter K, for different values of the wave number q.

namely, $q \in [0, 0.24]$. For this reason, in the present paper, we restrict to the wave number selected in such a finite interval, which correspond to biophysical situation of DNA molecule described in Ref. [44].

In doing so, the stationary soliton solution of Eq. (9) is

$$F_1(x,\tau) = A\,\mathrm{sech}[L(x-x_0)]e^{i\varpi(\tau-\tau_0)}, \tag{13}$$

where

$$A = u_e\sqrt{\frac{1-2\eta}{2PQ}}, \quad L = A\sqrt{\frac{Q}{2P}}, \quad \varpi = PL^2,$$

and $\eta = \frac{u_c}{u_e}$, with $\eta \in [0, 0.5]$. The parameters u_e and u_c are real numbers, which represent the envelope and carrier wave velocities, respectively. The constants x_0 and τ_0 are related to the initial conditions. The general solution for the out-of-phase motion Eq. (6b) is built by using Eqs. (7), (8), and (13), so that

$$\begin{aligned} v_n(t) = {} & 2A_\varepsilon\,\mathrm{sech}[L_\varepsilon(nr - v_g t)]\cos(qnr - \Omega t) \\ & + 2A_\varepsilon^2\,\mathrm{sech}^2[L_\varepsilon(nr - v_g t)] \\ & \times \left\{\frac{\mu}{2} + b\cos[2(qnr - \Omega t)]\right\} + 0(\varepsilon), \end{aligned} \tag{14}$$

where

$$A_\varepsilon = U_e\sqrt{\frac{1-2\eta}{2PQ}}, \quad L_\varepsilon = A_\varepsilon\sqrt{\frac{Q}{2P}}, \quad \Omega = \omega - \varpi_\varepsilon,$$

$$U_e = \varepsilon u_e, \quad \varpi_\varepsilon = PL_\varepsilon^2.$$

The parameters A_ε, L_ε, and Ω are the amplitude, inverse width, and angular frequency of the soliton, respectively. Experimentally observed in the DNA molecule, the soliton solution Eq. (14) represents a localized modulated wave also known as breather [46,47]. It describes the breathing mode in the DNA molecular chain. It represents the opening of few base pairs traveling along the molecule in the form of bubble with the velocity v_g. This is shown by the solid blue lines in Fig. 10.

In a coherent mode vibration for which the "effective" carrier and envelope velocities are assumed equal, i.e, $v_{xx} = \frac{\Omega}{q}$, the soliton solution $v_n(t)$ is a one-phase function. So, one obtains U_e as a function of η

$$U_e = \sqrt{\frac{4P(\omega - qv_g)}{1-2\eta}}. \tag{15}$$

The coherency of the soliton solution of the model is effective, so that the number N of the base pairs covered by a single soliton is known. As in Ref. [44], one assumes that N is integer

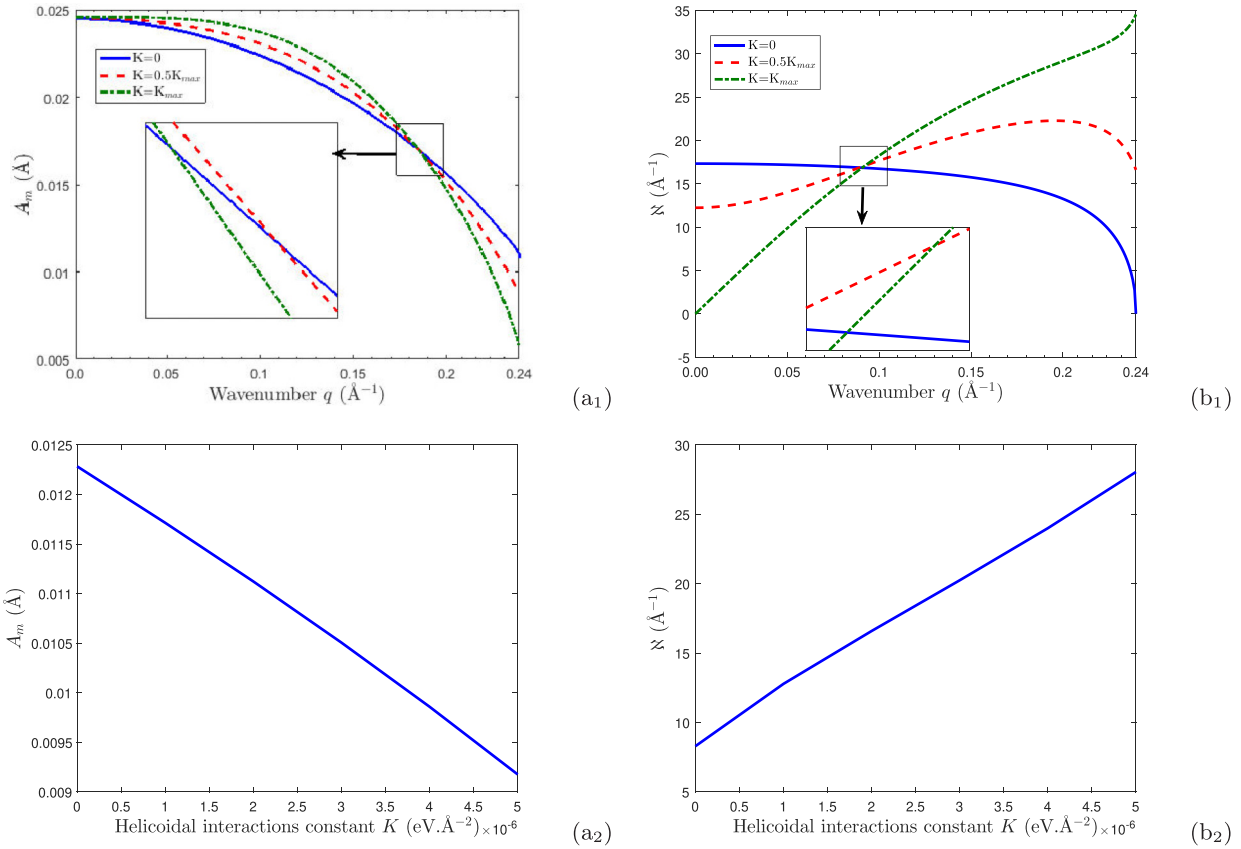

FIG. 2. Evolution of the amplitude A_m and width ℵ of the wave in the nonviscous and nonforced media. Panels (a_1) and (b_1), in terms of the wave number q, for different values of the helicoidal interactions constant. Panels (a_2) and (b_2), in terms of the helicoidal interactions constant K, for $q = 0.24$.

such that

$$N = \frac{2\pi}{qr}. \tag{16}$$

In this framework, for the wave number picked from the finite interval $0 \leqslant q < 0.24$ (Å^{-1}), one gets

$$N > 7. \tag{17}$$

This result is a range of the allowed values by Zdravković *et al.* [44]. They found that in the framework of the PBD model of DNA the number of opening base pairs should be $7 \leqslant N \leqslant 20$. Moreover, from Eq. (14), the "effective" amplitude A_m and width ℵ of the soliton can be expressed as

$$A_m = 2A_\varepsilon\left[1 + A_\varepsilon\left(\frac{\mu}{2} + BC\right)\right], \quad \text{and} \quad \aleph = \frac{2\pi}{L_\varepsilon}. \tag{18}$$

Figure 2 shows snapshots of the evolution of amplitude and width of the soliton solution in terms of the wave number, for different values of the helicoidal coupling constant K [see Figs. 2(a_1) and 2(b_1)] on one hand, and versus the later for $q = 0.24$ [see Figs. 2(a_2) and 2(b_2)] on the other hand. For the above, depending on the values of the wave number, the lines show that the amplitude and width are very sensitive to the change in the molecule helicity via K. More precisely, when the wave number $q = 0.24$, the amplitude of the soliton decreases and its width increases with increasing the helicoidal coupling. The lines in Figs. 2(a_2) and 2(b_2) of also show the linear evolution of both amplitude and width of the soliton when the helicoidal interactions evolve. While the amplitude decreases, the soliton width increases. That is, the higher the helicoidal interactions, the higher the number of base pairs in the bubble. In other words, the high values of the helicoidal interactions, which corresponds to a large number of stretched base pairs in the bubble, leads to a better representation of the open state configuration. It is also a better activator of energy for RNA-polymerase transport during the eventual opening of the DNA double helix, for bases to be exposed out of the stack. Moreover, when the helicoidal interaction constant takes small values, the wave is more localized. As the soliton is a mathematical instrument to represent breather mode in DNA, physically, it stands the opening of some base pairs moving in the form of bubble [46,47]. In such a context, a more localized solitonic wave may correspond to the opening of few base pairs in the bubble, experimentally observed during the leading DNA biological processes of transcription [48,49]. Similar observations were done in Ref. [23], in which the authors used a spin-like model of DNA. Showing that the impact of helical interactions on DNA behavior are independent on the model into consideration. Then, the soliton solution given in Eq. (39) can be a useful tool to describe the dynamics of open state configuration in the DNA molecule.

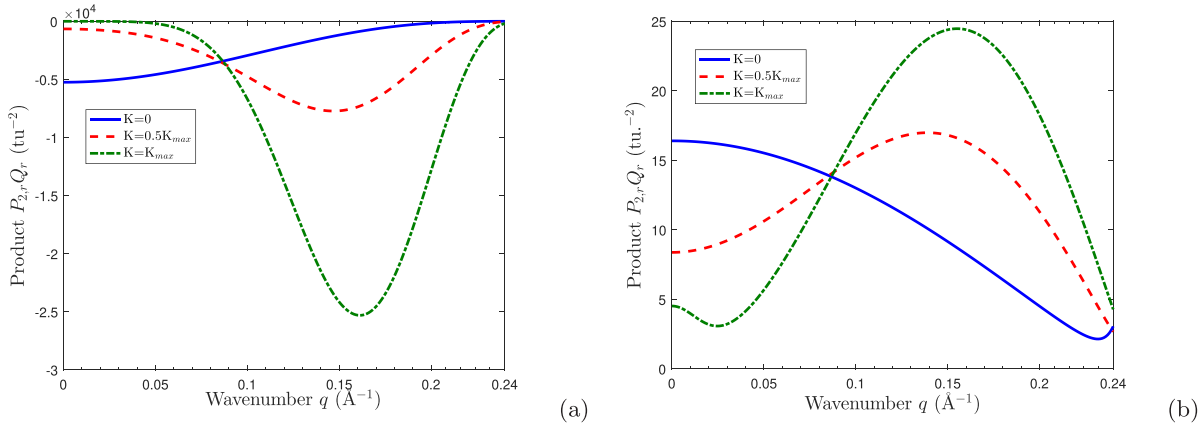

FIG. 3. Evolution of the product $P_{2,r}Q_r$ in terms of the wave number q, for different values of the helicoidal interactions constant, as the function of the chirp of the soliton. Panel (a) for $\sigma = \sigma_-$; panel (b) $\sigma = \sigma_+$.

III. IMPACT OF VISCOSITY AND EXTERNAL FORCE

A. Equation of motion: The complex Ginzburg-Landau equation

To protect the genetic information encoded in the bases buried inside the DNA structure, the dynamics of the molecule must be controlled. Usually, in mathematical physics, the control of the dynamics of a nonlinear system is done by investigating the effects of dissipation, noise, and external force on the system. Whereas dissipation leads to loss of energy and hence affects the dynamics of system, the external driving force behaves as a source of gain of energy, which helps in the stabilization the system [50,51].

In the last decades, nonlinear systems with external tunable driving forces attracted considerable attention because it can be observed in numerous physical systems such as the plasma driven by rf-fields, pulse propagation in twin-core fibers, charge density waves with external electric field, double-layer quantum Hall (pseudo) ferromagnets, DNA dynamics, and Josephson junction [52–56]. In addition, the external factors which generally lead to the driven (gain or loss) terms in the CGL (as well as in the NLS) equation are very important for their major role in controlling the diffusion induced amplitude and phase turbulence in the system [57–59].

Indeed, the DNA chain is not homogeneous and its environment known to be very noisy and inhomogeneous because of the differences between the bases along the chain, the presence of enzymes, particles of the solvent, and other chemical reactions, which lead to fluctuations in environmental conditions and the nonuniform medium. Thus, it makes the relevant parameters space and/or time dependent because external contributions and differences among bases affect the properties of the system change in space and/or time [60,61]. In doing so, for a good agreement with experimental observations, one must take into account DNA-environment interactions. Here, we discuss the case where the DNA-environment interactions can be reduced to dissipations or gain due to three different forces, the Stokes viscous forces, caused by the interactions between DNA nucleotides and particles of solvent [62], the hydrodynamical viscous forces caused by the hydrodynamics interactions between inner DNA nucleotides [57,58], and the external forces field due to inhomogeneities, and additional molecules or external agents [8,63].

In recent studies on the dynamical properties of some physical systems in the presence of external forces field, the case of constant forces [64], periodic forces [64–66], or cubic anharmonic forces [67] were considered. However, since the external factors strongly depend on time [60,61], in the present study, we extend the above-mentioned studies by assuming the external forces in the form of nonlinear function of a high degree of damping [68].

The realistic equation of motion is obtained by adding the Stokes viscous forces $F^{\rm St} = -\gamma^{st}\dot{v}_n^{(-)}$, the hydrodynamics viscous forces $F^{hy} = \gamma^{hy}(2\dot{v}_n - \dot{v}_{n+1} - v_{n-1})$, and the external forces $F^{\rm ex} = k_0 v_n + k_1 \dot{v}_n + k_2 \ddot{v}_n$ to the right-hand side of Eq. (6b). The real positive constants k_0, k_1, and k_2 have the dimension of a helicoidal or stacking interaction constant, a viscosity constant, and a mass, respectively. The parameters $\gamma^{\rm st}$ and $\gamma^{\rm hy}$ are the Stokes damping constant and hydrodynamical damping coupling constant, respectively. As in Ref. [69], we assume $\gamma^{\rm St} = \gamma^{\rm hy}$. Considering all the above, i.e., various growth and damping forces, the studied model [see Eq. (6b)] becomes

$$\begin{aligned}\ddot{v}_n =& J[(v_{n+1} - v_n) + (v_{n-1} - v_n)] \\ &- K[(v_{n+h} + v_n) + (v_{n-h} + v_n)] \\ &- S[(v_{n+1} - v_n)^3 + (v_{n-1} - v_n)^3] \\ &- \omega_g^2\left(v_n + \alpha v_n^2 + \beta v_n^3\right) \\ &- \gamma^{St}\dot{v}_n + \gamma^{hy}(\dot{v}_{n+1} - 2\dot{v}_n + \dot{v}_{n-1}) \\ &+ k_0 v_n + k_1 \dot{v}_n + k_2 \ddot{v}_n. \end{aligned} \tag{19}$$

Equation (19) is a nonlinear differential-difference equation, which describes the transverse out-of-phase motions of the DNA molecular chain in an external force field, taking into the Stokes and hydrodynamics viscous forces.

To apply the above-mentioned multiple scale approximation method, one assumes the soliton solution on the form

$$\begin{aligned} v_n =& \varepsilon[F_{n,1,\gamma} e^{i\theta_{n,\gamma}} + F_{n,1}^* e^{-i\theta_{n,\gamma}}] \\ &+ \varepsilon^2[F_{n,0,\gamma} + (F_{n,2,\gamma} e^{2i\theta_{n,\gamma}} + F_{n,2,\gamma}^* e^{-2i\theta_{n,\gamma}})], \end{aligned} \tag{20}$$

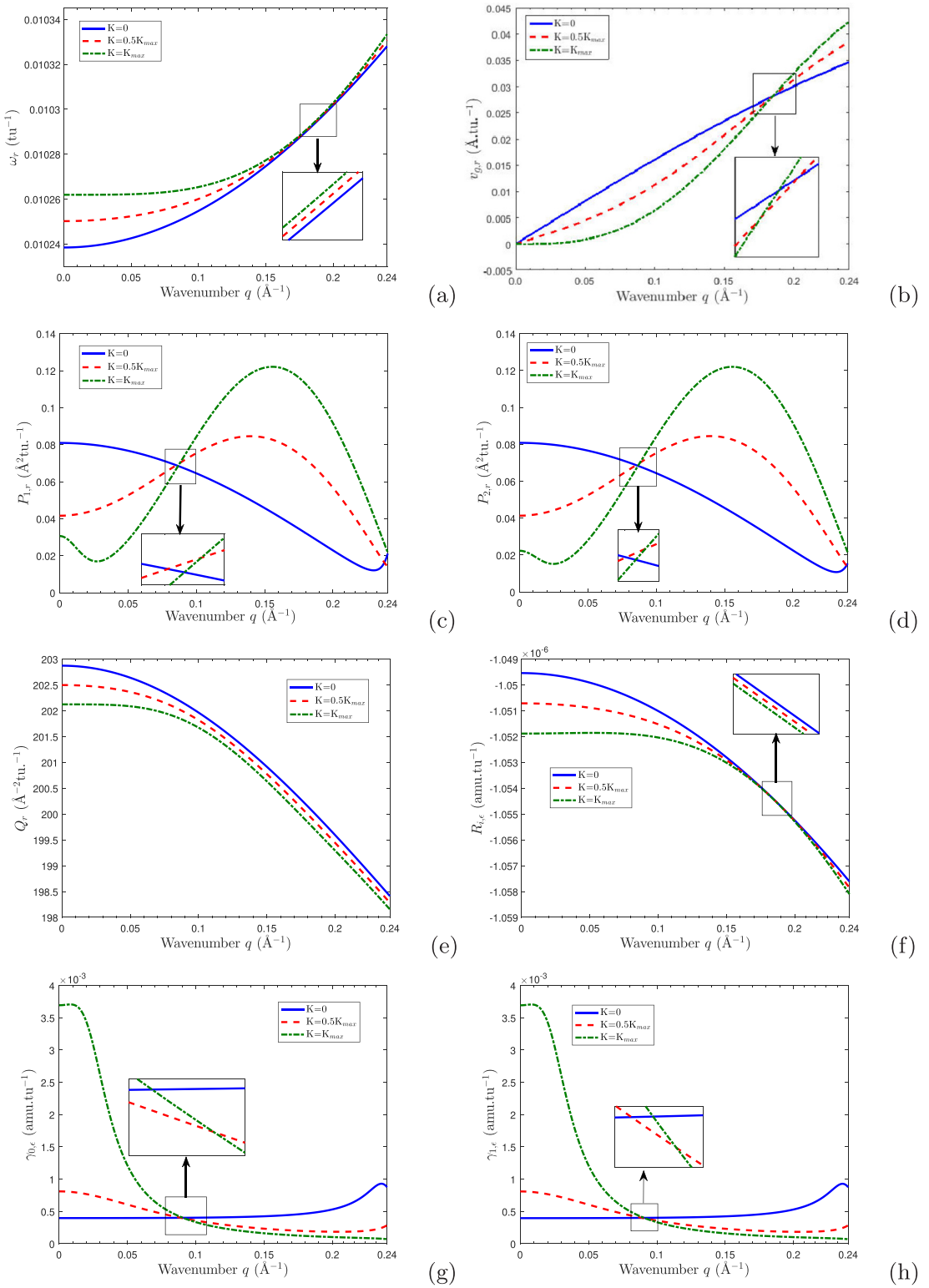

FIG. 4. Panels (a)–(h) represent the evolution of the angular frequency ω_r, the group velocity $v_{g,r}$, the "dispersion" coefficients $P_{1,r}$ and $P_{2,r}$, the nonlinearity coefficient Q_r, the loss or gain parameters $R_{i,\varepsilon}$, $\gamma_{0,\varepsilon}$, and $\gamma_{1,\varepsilon}$ of the wave in the viscous and forced medium, in terms of the wave number q, for different values of the helicoidal interactions constant, respectively.

where $\theta_{n,\gamma} = qrn - \omega_\gamma t$, the phase of the soliton in the heavy damped medium, ω_γ the complex angular frequency of the base pairs vibrations.

In addition, we assume weak interactions between the external forces field and the DNA molecule. Indeed, their contributions are assumed little enough to the whole DNA dynamics, which is dominated by the other nonlinear terms in the equation of motion [64]. Therefore, the external forces are considered to be perturbed at the order ε^2 [8,38]. The numerical values of additional parameters used are $\gamma^{\mathrm{St}} = \gamma^{\mathrm{hy}} = 0.5$

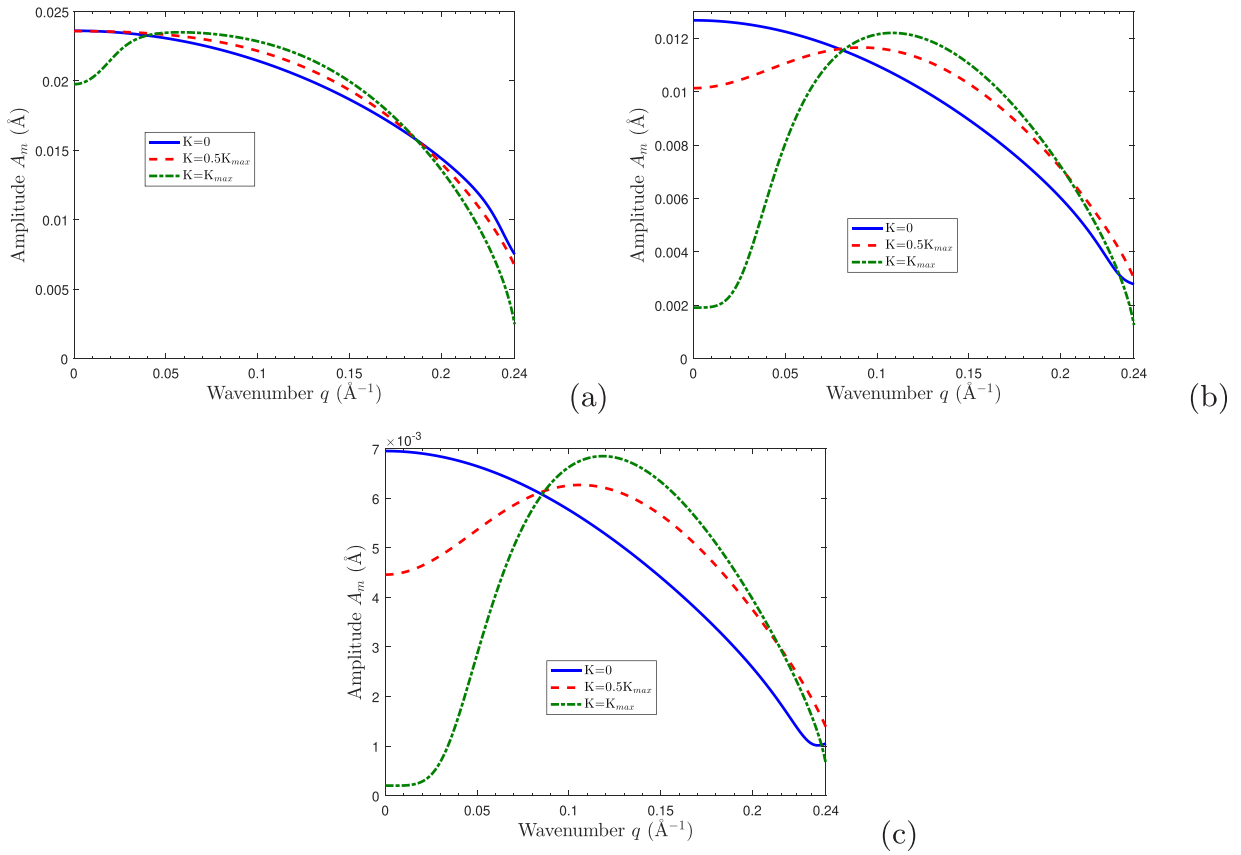

FIG. 5. Evolution of the amplitude $A_{\gamma,m}(t)$ of the soliton propagating in the viscous media, in terms of wave number q for different values of the helicoidal interactions constant K, at different time (a) $t = 0$ tu, (b) $t = 500$ tu, and (c) $t = 1000$ tu.

tu^{-1}, $\epsilon = 0.01$, and $k_0 = k_1 = k_2 = 1$. Additionally, the functions F_0 and F_2 are found as

$$F_{0,\gamma} = \mu|F_{1,\gamma}|^2, \quad F_{2,\gamma} = b_\gamma F_{1,\gamma}^2, \tag{21}$$

with

$$\begin{aligned} b_\gamma &= B_1C_1 + iD_1C_1, \quad B_1 = 4\omega_r^2 - \varsigma, \\ C_1 &= \frac{\omega_g^2\alpha}{B_1^2 + D_1^2}, \quad D_1 = 4\chi\omega_r, \\ \chi &= \frac{\gamma}{2}, \quad \gamma = \gamma^{st} + 4\gamma^{hy}\sin^2(qr/2), \end{aligned} \tag{22}$$

where μ and ς are given in Eq. (11). Moreover, the function $F_{1,\gamma}(x,\tau)$ is the slowly varying envelope soliton solution of the following equation:

$$i\frac{\partial F_{1,\gamma}}{\partial\tau} + P_\gamma\frac{\partial^2 F_{1,\gamma}}{\partial x^2} + Q_\gamma|F_{1,\gamma}|^2F_{1,\gamma} + R_\gamma F_{1,\gamma} = 0, \tag{23}$$

where

$$P_\gamma = P_r + iP_i, \quad Q_\gamma = Q_r + iQ_i, \quad R_\gamma = R_r + iR_i,$$

with

$$\begin{aligned} P_r &= \frac{1}{\omega_r}[r^2(J - \chi\gamma^{hy})\cos(qr) \\ &\quad - K(rh)^2\cos(qrh) - |v_g|^2], \\ P_i &= -\frac{1}{2}r^2\gamma^{hy}\cos(qr), \end{aligned}$$

$$\begin{aligned} Q_r &= -\frac{\omega_g^2\alpha}{\omega_r}\left[\mu + \frac{3}{2}\beta/\alpha + B_1C_1\right] \\ &\quad + \frac{6S}{\omega_r}[1 - \cos(qr)]^2, \\ Q_i &= -\frac{\omega_g^2\alpha}{\omega_r}C_1D_1, \\ R_r &= -k_0 + k_1\chi + k_2\left(\omega_r^2 - \chi^2\right), \\ R_i &= -(k_1 - 2k_2\chi)\omega_r. \end{aligned} \tag{24}$$

The angular frequency and group velocity are given by

$$\begin{aligned} &\omega_\gamma = \omega_r + i\omega_i, \quad \omega_r = \omega\sqrt{1-\delta^2}, \quad \omega_i = -\chi, \ \delta = \frac{\chi}{\omega}, \\ &v_g = v_{g,r} + iv_{g,i}, \quad v_{g,i} = -r\gamma^{hy}\sin(qr), \\ &v_{g,r} = \frac{r}{\omega_r}[(J - \chi\gamma^{hy})\sin(qr) - Kh\sin(qrh)], \end{aligned} \tag{25}$$

where ω is the angular wave frequency for the linear modes in absence of damping, which corresponds to the nonviscous and nonforced limit given in Eq. (12). The subscripts r and i are related, respectively, to the real and imaginary parts of the parameter into consideration. Meanwhile, the damping introduces an imaginary component of the frequency, i.e., an exponential decay of the amplitude.

Equation (23) is the CGL equation governing the dynamics of the heavy damped DNA molecule in a weak external forces

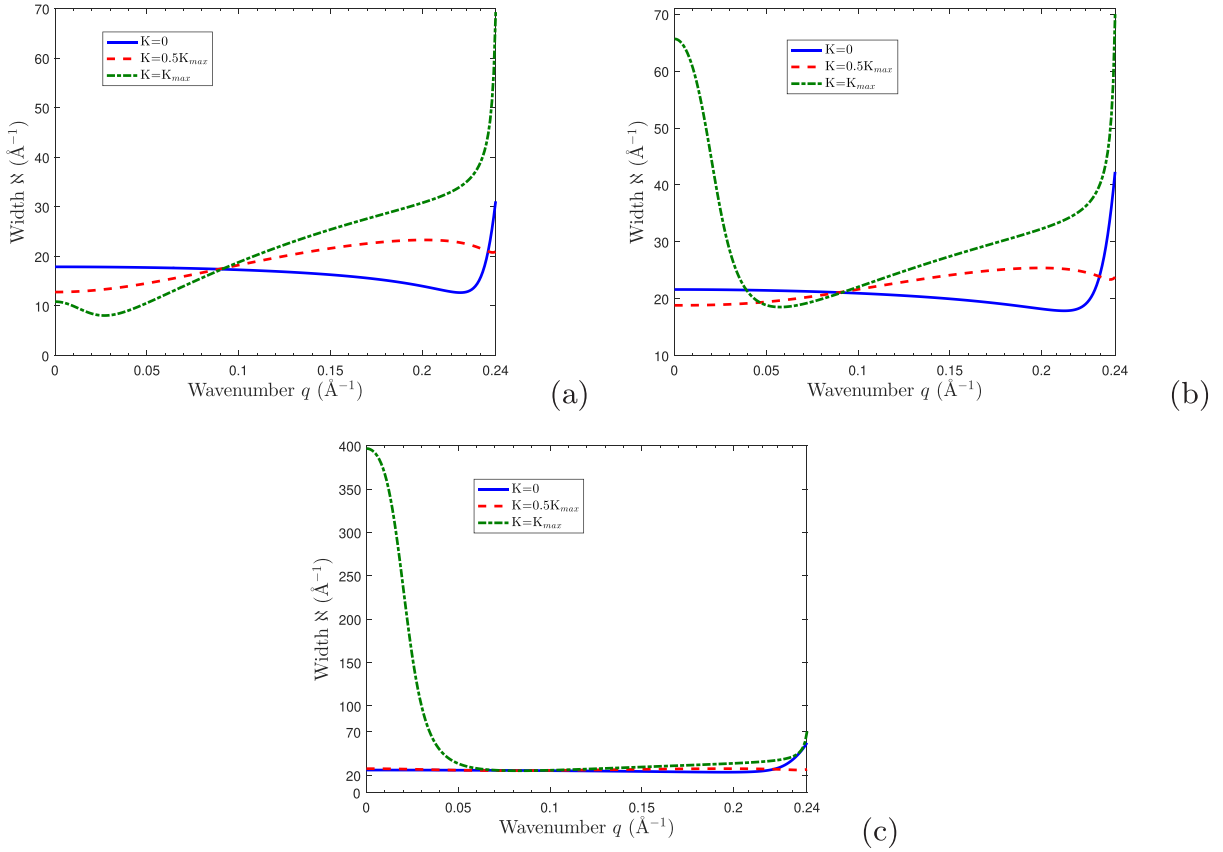

FIG. 6. Evolution of the width $\aleph_\gamma(t)$ of the soliton propagating in the viscous media, in terms of wave number q for different values of the helicoidal interactions constant K, at different time (a) $t = 0$ tu, (b) $t = 500$ tu, and (c) $t = 1000$ tu.

field. Also viewed as a dissipative extension of the conservative NLS equation, the CGL equation introduced seventy years ago by Ginzburg and Landau [70] is one of the most universal equations of modern physics. Particularly, its describes with good accuracy the dissipative nonlinear systems, which typically involve gain and loss of matter or energy [71–73]. The CGL equation either in their original or modified forms describe on a qualitative, and often even on a quantitative level a wealth of phenomena and systems, from different branches of physics to biology [74,75]. For example, if $P_i \approx Q_i \approx R_r \approx 0$, the CGL equation becomes the dissipative NLS equation or Standard NLS equation (if also $R_i = 0$). When $P_r \approx Q_r \approx R_r \approx 0$, it becomes the real Ginzburg-Landau (GL) equation, and when $P_r \approx P_i \approx 0$, it is reduced to the complex Landau equation or real Landau equation (if also $Q_r \approx R_r \approx 0$). Based on the Ginzburg-Landau (GL) theory, which is an extension of the Landau [76] theory of second-order phase transitions into the quantum phenomenon of superconductivity, the CGL equation was one of the first nonlinear theories to show solutions in the form of topological singularities. Physically, the GL theory was based on the idea that in the absence of a magnetic field, the normal metal-superconducting state transition is a thermodynamic second-order transition.

Physically, in Eq. (23), the function $F_{1,\gamma}(x,\tau)$ represents the normalized envelope of the base pairs stretching, with $x = \varepsilon(z - v_{g,r}t)$ and $\tau = \varepsilon^2 t$, the scaled space and time coordinates, respectively. The parameters P_r and Q_r represent the dispersion and nonlinearity coefficients, respectively. In fact, the interplay between the nonlinearity Q_r, which determines how the wave frequency is amplitude modulated, and dispersion P_r, which measures the wave dispersion, is responsible for the occurrence of solitons. The cubic nonlinearity damping terms Q_i measures the saturation of the unstable wave, while the gain bandwidth coefficient P_i measures the relative growth rate of perturbations whose spectra is concentrated near the fundamental wave number q. The parameters R_r and R_i are frequency shifted coefficients and the linear gain or loss, respectively.

Seen also as perturbation terms of the standard NLS equation, the linear gain coefficient R_γ, the imaginary parts of the dispersion coefficient P_i and nonlinearity coefficient Q_i, come from the external forces, the hydrodynamics and Stokes viscous forces, respectively. Since these additional terms are not zero, Eq. (23) is not integrable, contrary to its counterpart the standard NLS equation, which is completely integrable but not applicable to the powerful physics situations described by the CGL (as well as the modified NLS) equation.

For instance, since the nature generally selects inhomogeneous DNA molecules moving in noisy crowded environment, the CGL (as well as the modified NLS) equation is well adapted to describe the real dynamics of DNA systems. It is well known that DNA is made of charged phosphate groups along the strands, which interact through dipole-dipole long-range interactions (LRI) [17]. Moreover, the DNA environment is usually a biological fluid with very active biological entities such as enzymes, proteins, or other molecules,

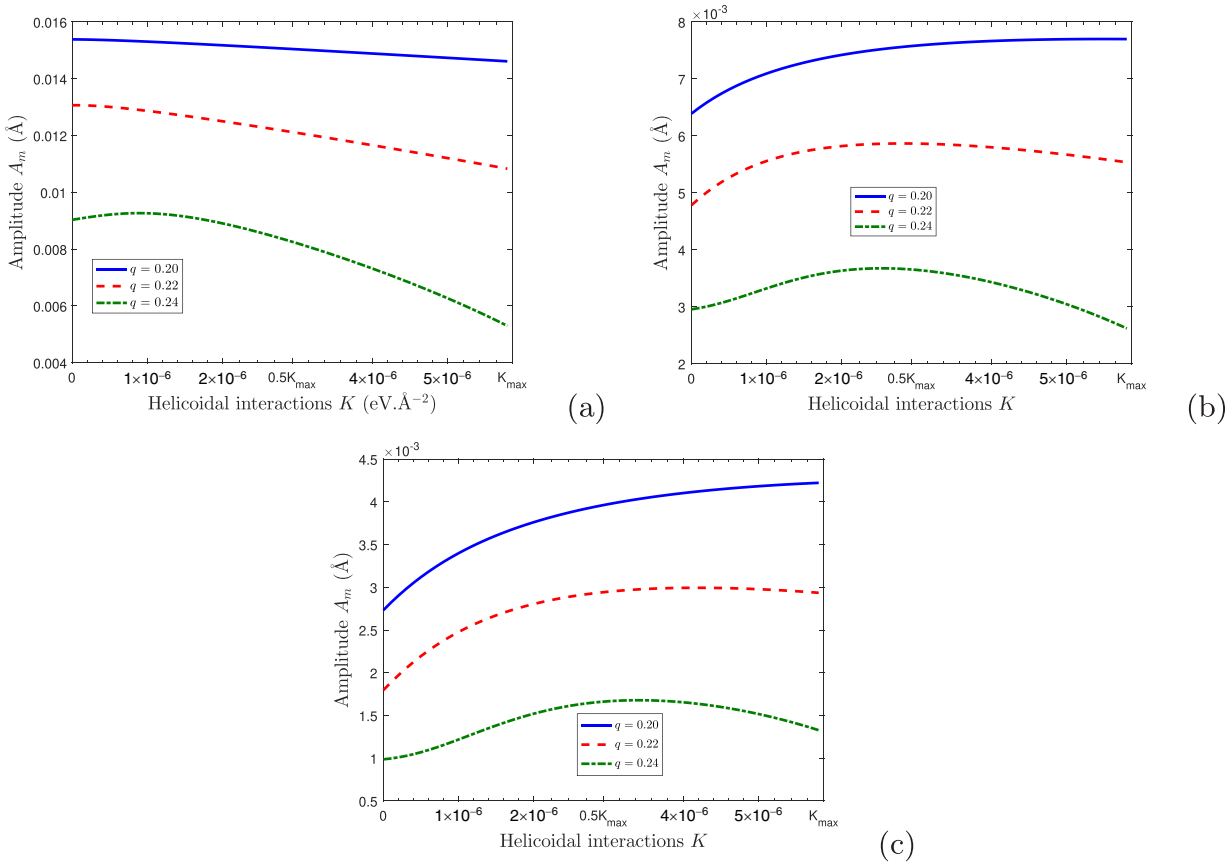

FIG. 7. Evolution of the amplitude $A_{\gamma,m}(t)$ of the soliton solution propagating in the viscous media, in terms of the helicoidal interactions constant K, at three times, namely, $t = 0$ tu, $t = 500$ tu, and $t = 1000$ tu.

which cause Stokes damping [62], hydrodynamics damping [57,58], inhomogeneities or external potential field [8–10], or memory effects [20] on the dynamical behaviors of DNA molecule.

Contrary to the NLS equation for which the solution are conservative solitons, the solutions of CGL equation are dissipative solitons, which usually exist during a limited lifetime before eventually vanishing. Their existence are due to the composite interplays of nonlinear or linear loss and amplification, along with dispersion and the nonlinearity coefficient, provides mechanisms to generate solitons that do not decay [74,77–79]. The characteristics of dissipative solitons are determined by the coefficients of the evolution equation. So, they do not exist as families of solutions as in the case of conservative soliton solutions [74]. Thus, only exact soliton solutions related to the mathematical tools used and problems on interest can be obtained.

In the quest for dissipative solitons, exact solutions play an important role as they provide some remarkable mechanisms to the understanding the formation of solitons in numerous physical dissipative systems. It is a challenge to search for exact dissipative soliton solutions because it can give rise to new scenarios to establish double balances in dissipative nonlinear systems, and opens the route toward more new dissipative solitonic structures.

To investigate the impact of the mass inhomogeneities and external one-site potential on the soliton solution, the similarity transformation method was recently used [63,80] and relevant results obtained. Also, the effects of the localized and exponential stacking interaction inhomogeneities on the amplitude, width, velocity, and phase of the moving soliton, were successfully investigated with the aid of the perturbation technique [8]. More recently, the lightly damping effects on the amplitude and width of the open-state configuration, describing the dynamical behaviors of DNA molecule in a weakly dissipative medium was discussed [38].

B. Exact analytical bright-like soliton solutions of the complex Ginzburg-Landau equation

The mathematical approach in this work was used successfully in a couple of works [29,38,81] among which Kengne *et al.* [29] exclusively applied it to a dissipative NLS equation. This was further extended to more complex problems involving the cubic CGL equation not only in electrical lattices and in nonlinear microtubule RLC transmission line, but also in the nonlinear dynamics of DNA molecule in the weakly dissipative medium [38,81].

In the works mentioned above [29,38,81], the analysis deals with the NLS equation with additional dissipative terms. In this part, we exclusively implement the technique in the description of dynamical properties of a physical systems governed by a CGL equation. For this, the following ansatz is introduced:

$$F_{1,\gamma}(x,\tau) = f(\tau)\psi(X)e^{i[K_1 x + g(\tau)]}, \tag{26}$$

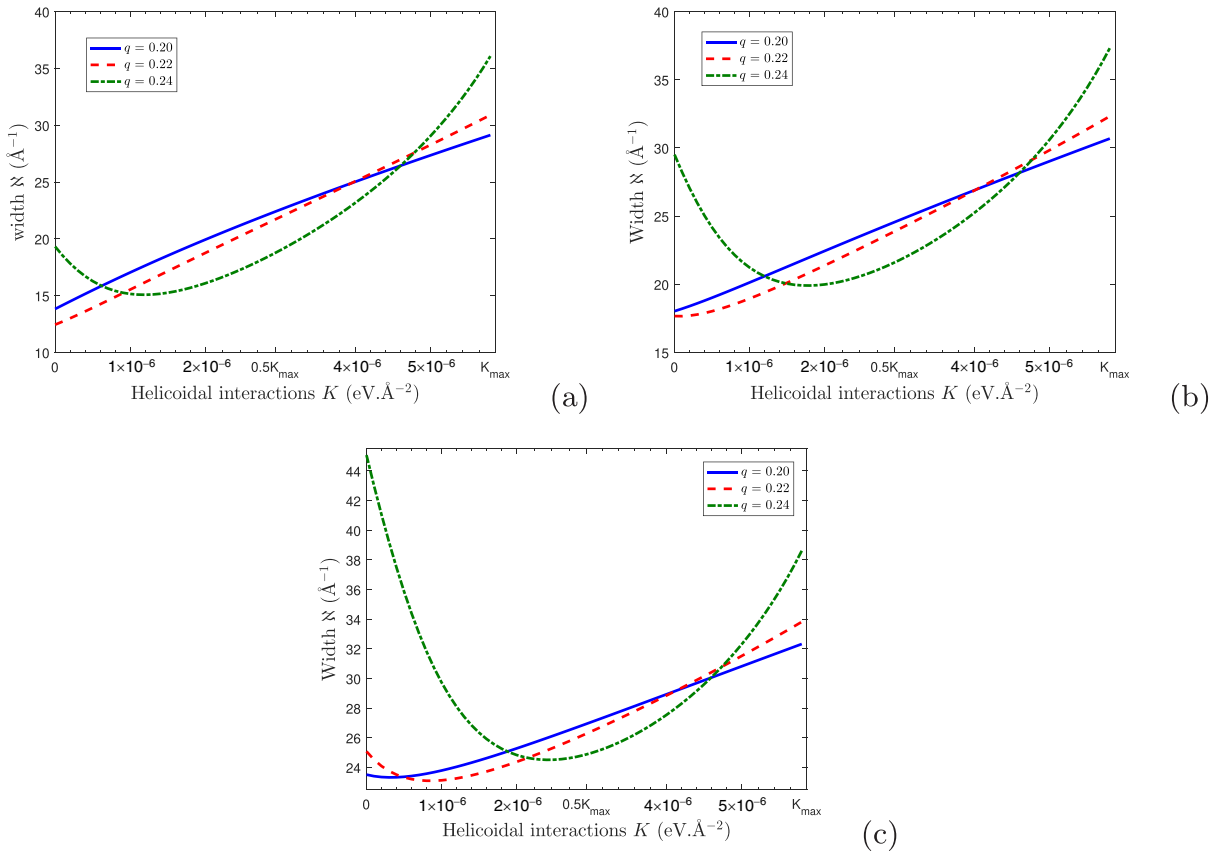

FIG. 8. Evolution of the width $\aleph_\gamma(t)$ for the soliton propagating in the viscous media, in terms of the helicoidal interactions constant K, at three times, namely, (a) $t = 0$ tu, (b) $t = 500$ tu, and (c) $t = 1000$ tu.

where

$$X(x,\tau) = a_0(\tau)x + b_0(\tau). \tag{27}$$

The functions $f(\tau)$, $g(\tau)$, $a_0(\tau)$, and $b_0(\tau)$ are real functions of variable τ, while ψ is a complex function of variable X. The real numbers K_1 and $\frac{dg(\tau)}{d\tau}$ are the wave number and the angular frequency, respectively. The functions $f(\tau)$, $a_0(\tau)$, and $\frac{b_0(\tau)}{a_0(\tau)}$ are related to the amplitude, inverse width, and initial position of the soliton. Inserting Eq. (26) in Eq. (23) yields

$$\begin{aligned} & i\frac{1}{f}\frac{\partial f}{\partial \tau}\psi + i\left[\frac{X}{a_0}\frac{\partial a_0}{\partial \tau} - \frac{b_0}{a_0}\frac{\partial a_0}{\partial \tau} + \frac{\partial b_0}{\partial \tau}\right]\frac{\partial \psi}{\partial X} - \frac{\partial g}{\partial \tau}\psi \\ & + (P_r + iP_i)\left[a_0^2\frac{\partial^2\psi}{\partial X^2} - K_1^2\psi + 2iK_1a_0\frac{\partial \psi}{\partial X}\right] \\ & + (Q_r + iQ_i)f(\tau)^2|\psi|^2|\psi| + (R_r + iR_i)\psi \\ & = 0. \end{aligned} \tag{28}$$

We should remember that the equation for which we are looking for a soliton solution is a CGL equation. So, in the following, the complex function $\psi(X)$ is assumed as [82,83]

$$\psi(X) = [\varphi(X)]^{1+i\sigma}, \tag{29}$$

where the constant σ appears as the chirp of the soliton to be determined. The terms $\varphi(X)^{i\sigma}$ represents the X-dependent phase of the soliton. Inserting Eq. (29) and its derivatives into Eq. (28) leads to

$$\begin{aligned} & \left[i\frac{1}{f}\frac{\partial f}{\partial \tau} - \frac{\partial g}{\partial \tau} + (R_r + iR_i) - (P_r + iP_i)K_1^2\right]\varphi \\ & + i(1+i\sigma)\left[\frac{X}{a_0}\frac{\partial a_0}{\partial \tau} - \frac{b_0}{a_0}\frac{\partial a_0}{\partial \tau} + \frac{\partial b_0}{\partial \tau}\right. \\ & \left. + 2(P_r + iP_i)K_1a_0\right]\frac{\partial \varphi}{\partial X} + (P_r + iP_i)(1+i\sigma)a_0^2 \\ & \times\left[\frac{\partial^2\varphi}{\partial X^2} + i\sigma\left(\frac{\partial \varphi}{\partial X}\right)^2\varphi^{-1}\right] + (Q_r + iQ_i)f^2\varphi^3 \\ & = 0. \end{aligned} \tag{30}$$

To further proceed, we impose that the coefficient of the terms $\frac{\partial \varphi}{\partial X}$ must vanish. Accordingly, we have

$$\frac{X}{a_0}\frac{\partial a_0}{\partial \tau} - \frac{b_0}{a_0}\frac{\partial a_0}{\partial \tau} + \frac{\partial b_0}{\partial \tau} + 2(P_r + iP_i)K_1a_0 = 0. \tag{31}$$

Equation (31) is always satisfied if and only if all its coefficients are all zero. So that we have $K_1 = 0$, while a_0 and b_0 are constant real numbers. Thus, we assume that they are proportional. For instance we assume $\frac{b_0}{a_0} = -x_0$, with x_0 a real number related to the initial position of the soliton. Therefore, one obtains

$$X(x,\tau) = a_0(x - x_0), \tag{32}$$

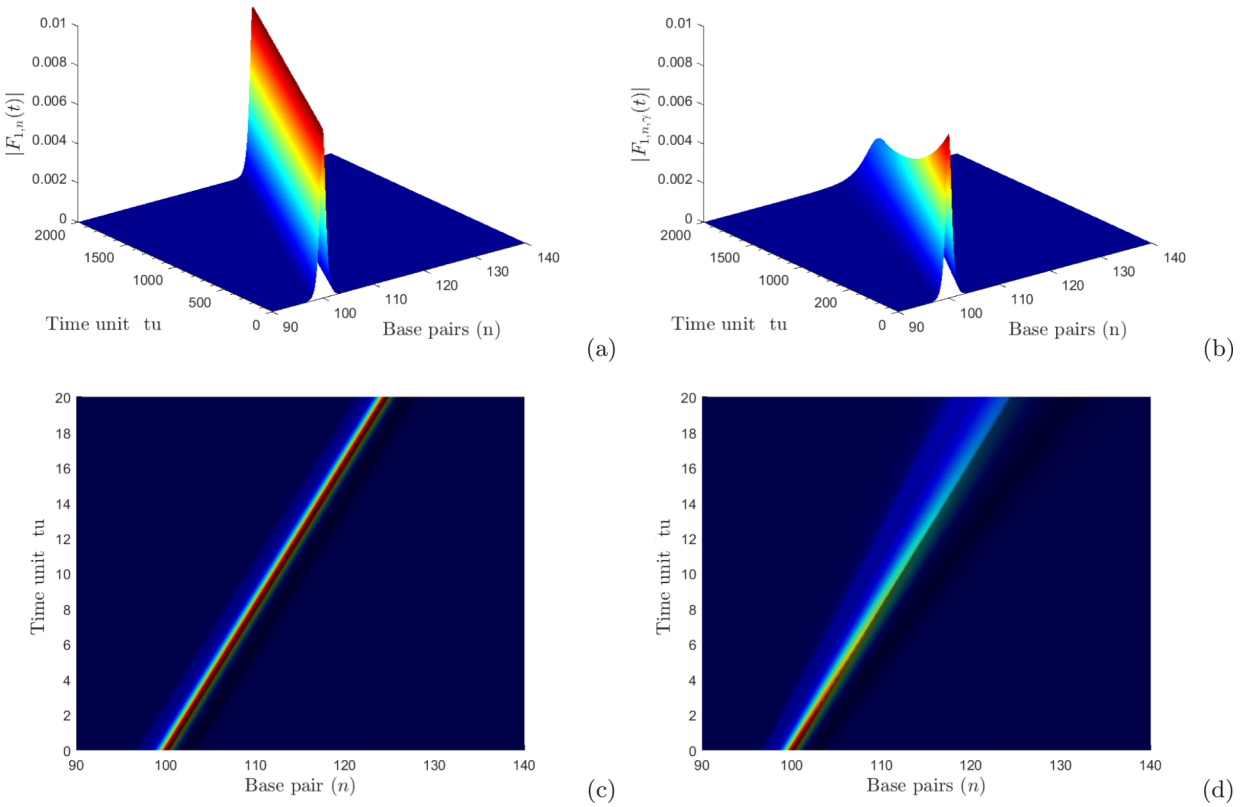

FIG. 9. Comparison between numerical 3D simulations of the envelope soliton, for $K = K_{\max}$ and $u_e = 0.1$ Å tu^{-1}. Panels (a) and (c): The nonviscous and nonforced case. Panels (b) and (d): The viscous case.

and Eq. (30) becomes

$$\left[i\frac{1}{f}\frac{\partial f}{\partial \tau} + (R_r + iR_i) - \frac{\partial g}{\partial \tau}\right]\varphi + (P_r + iP_i)(1 + i\sigma)a_0^2\left[\frac{\partial^2 \varphi}{\partial X^2} + i\sigma\left(\frac{\partial \varphi}{\partial X}\right)^2 \varphi^{-1}\right] + (Q_r + iQ_i)f^2\varphi^3 = 0. \tag{33}$$

From the above, one can seen that depending on the wave-like functions used, the CGL equation can be solved for different types of soliton-like solutions, such as bright-like, dark-like, or kink-like soliton solutions. Meanwhile, the type of soliton-like solution of Eq. (23) is controlled by Eq. (33). That is, any solitary wave-like solution of Eq. (33) gives a soliton-like solution of the CGL Eq. (23).

In the following, we restrict ourselves to bright-like soliton solution of the bell shape with a pulse near $x = x_0$, and a vanishing amplitude at $|x| \to \infty$, which represents an open-state configuration in an individual strand of DNA. In fact, such a solution has the appropriate profile to represent breathing modes in DNA. Therefore, we look for the soliton solution of Eq. (33) in the form

$$\varphi(X) = \operatorname{sech}[mX], \tag{34}$$

where m^{-1} is related to the width of the soliton. Then, we introduced Eq. (34) and its derivatives into Eq. (33). After canceling the terms in $\operatorname{sech}[mX]$, the functions $f(\tau)$ and $g(\tau)$ yield

$$g(\tau) = \varpi_\gamma(\tau - \tau_0), \quad f(\tau) = e^{-\gamma_1(\tau-\tau_0)}, \tag{35}$$

where

$$\varpi_\gamma = \varpi_0 + R_r, \quad \gamma_1 = \gamma_0 + R_i,$$

with

$$\varpi_0 = P_{1,r}L_0^2, \quad P_{1,r} = P_r - \sigma[2P_i + \sigma P_r],$$
$$\gamma_0 = P_{1,i}L_0^2, \quad P_{1,i} = P_i + \sigma[2P_r - \sigma P_i].$$

The parameters $L_0 = a_0 m_0$ and τ_0 are the initial inverse width of the soliton and initial time, respectively. The parameter γ_1 is a gain or loss terms, its comes from both damping and external forces.

The canceling of the terms in $\operatorname{sech}^3[mX]$ yields

$$L_0 = \sqrt{\frac{Q_r}{2P_{2,r}}}f_0, \quad L(\tau) = \sqrt{\frac{Q_r}{2P_{2,r}}}f(\tau), \tag{36}$$

where

$$P_{2,r} = P_r - \frac{1}{2}\sigma[3P_i + \sigma P_r], \quad \text{and} \quad \sigma_\pm = \frac{-b \pm \sqrt{\Delta}}{2a},$$

with

$$a = P_rQ_i - P_iQ_r, \quad b = 3(P_rQ_r + P_iQ_i),$$
$$c = 2(P_iQ_r - P_rQ_i), \quad \Delta = b^2 - 4ac, \; P_{2,r}Q_r > 0.$$

The constant f_0, related to the initial amplitude of the soliton is to be determined.

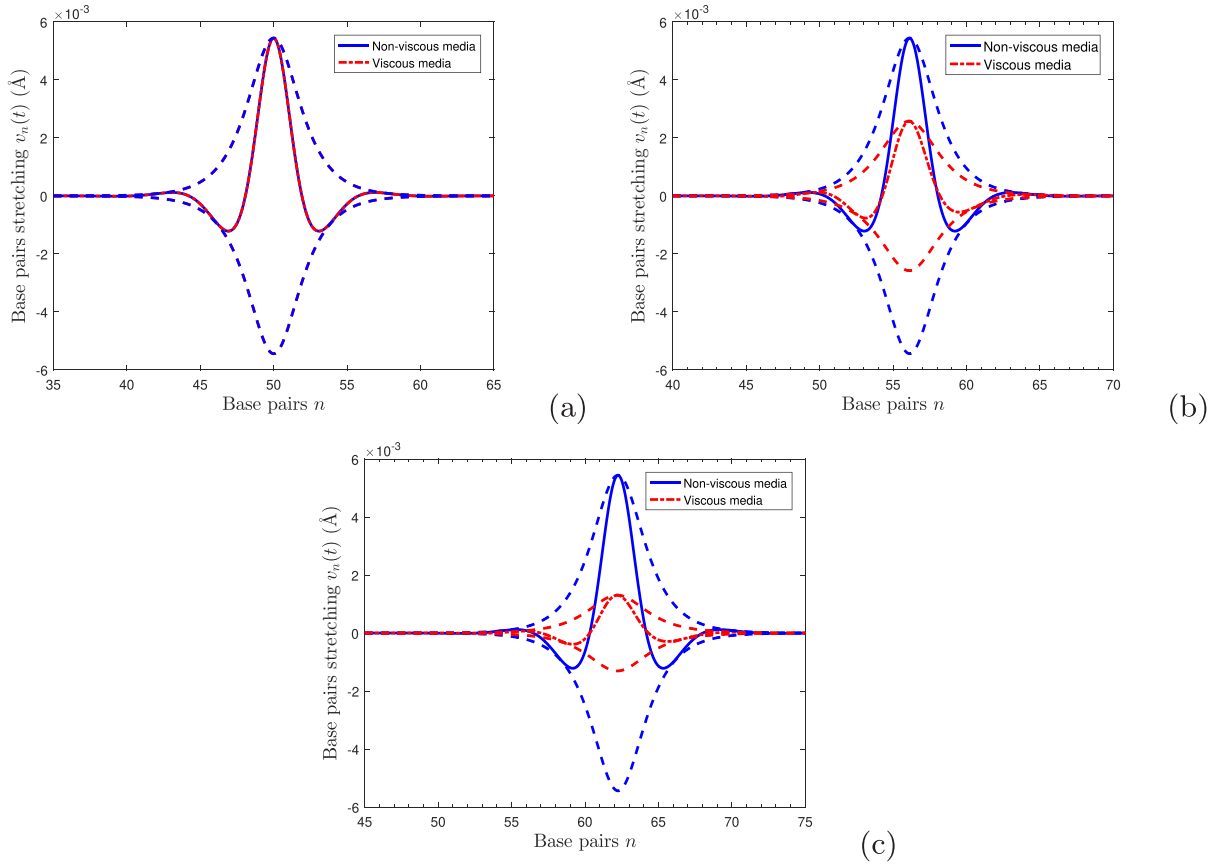

FIG. 10. Comparison between numerical simulations of the stretching nucleotide pairs in the viscous and nonviscous and nonforced media, at three times, namely, (a) $t = 0$ tu, (b) $t = 500$ tu, and (c) $t = 1000$ tu. For $K = K_{\max}$. Solid Blue line represents the soliton propagation in the nonviscous and nonforced medium, while the dash-dotted red line show the propagation in the viscous and forced media.

In our investigation, we found that when the chirp of the soliton is σ_-, the product $P_{2,r}Q_r$ is always negative [see Fig. 3(a)], and when this chirp is σ_+, this product is always positive [see Fig. 3(b)]. Consequently, in the following, we impose $\sigma = \sigma_+$, for which the soliton will be strongly chirped.

In Fig. 4, we plotted some solitonic parameters such as the angular frequency ω_r, the group velocity $v_{g,r}$, the "dispersion" coefficients $P_{1,r}$ and $P_{2,r}$, the nonlinearity coefficient Q_r, the loss or gain parameters $\gamma_{0,\varepsilon}$, $R_{i,\varepsilon}$, and $\gamma_{1,\varepsilon}$ versus the wave number q, for different values of the helicoidal interactions constant. It is obvious that all the above solitonic parameters are positive except the linear $R_{i,\varepsilon}$, which is negative. Thus, the parameter γ_0, which is a consequence of viscosity acts as a damping terms, while the parameter $R_{i,\varepsilon}$ which comes from the external forces acts as a growth terms for the systems. Specifically, while the viscosity makes the amplitude of the soliton to damp out, the external forces put energy on it, and hence increases the life time of the soliton in the DNA molecular structure. Furthermore, the parameter $\gamma_{1,\varepsilon}$ is positive. Accordingly, it behaves as a damping term. Also, as stated above, one observes that depending on the value of the wave number q, except the angular frequency which increases, and the nonlinearity and linear gain coefficients which decrease with the increasing of the helicoidal coupling constant, the others parameters increase, decrease or remain constant.

The soliton solution of the CGL equation is obtained from Eqs. (26) to (36) as

$$F_{1,\gamma}(x,\tau) = f(\tau)\,\mathrm{sech}[L(\tau)(x - x_0)]^{1+i\sigma}\, e^{i\varpi_\gamma(\tau-\tau_0)}, \quad (37)$$

where

$$f(\tau) = f_0 e^{-\gamma_1(\tau-\tau_0)}, \quad L(\tau) = L_0 e^{-\gamma_1(\tau-\tau_0)}.$$

Equation (37) is a dissipative soliton solution of the envelope wave equation Eq. (23). It is a nonlinear localized soliton solution of a nonconservative class, equivalent to those found in Refs. [82,83]. Moreover, the terms $e^{-\gamma_1(\tau-\tau_0)}$ enter in the amplitude and width of the soliton that can increase or decrease these parameters depending on the range of variation of the "the parameter" γ_1. More clearly, if $\gamma_1 > 0$, the wave amplitude decays with time showing that the system losses energy, and if $\gamma_1 < 0$ the wave amplitude grows as the wave propagates, showing that the system gains energy.

Contrary to the NLS equation for which the wave amplitude decays in response to dissipation, the dissipative solution of the CGL equation does not automatically decay, the system is active and consumes or gains energy. Thus, the soliton amplitude (as well as the width) of the soliton can decay or increases.

In the absence of damping and external forces, the dispersion and nonlinearity coefficients of both systems are equal, i.e., $P_{1,r} = P_{2,r} = P_r = P$, and $Q_r = Q$. Then, at the initial time $\tau = \tau_0$, the stationary soliton solutions given by Eqs. (37)

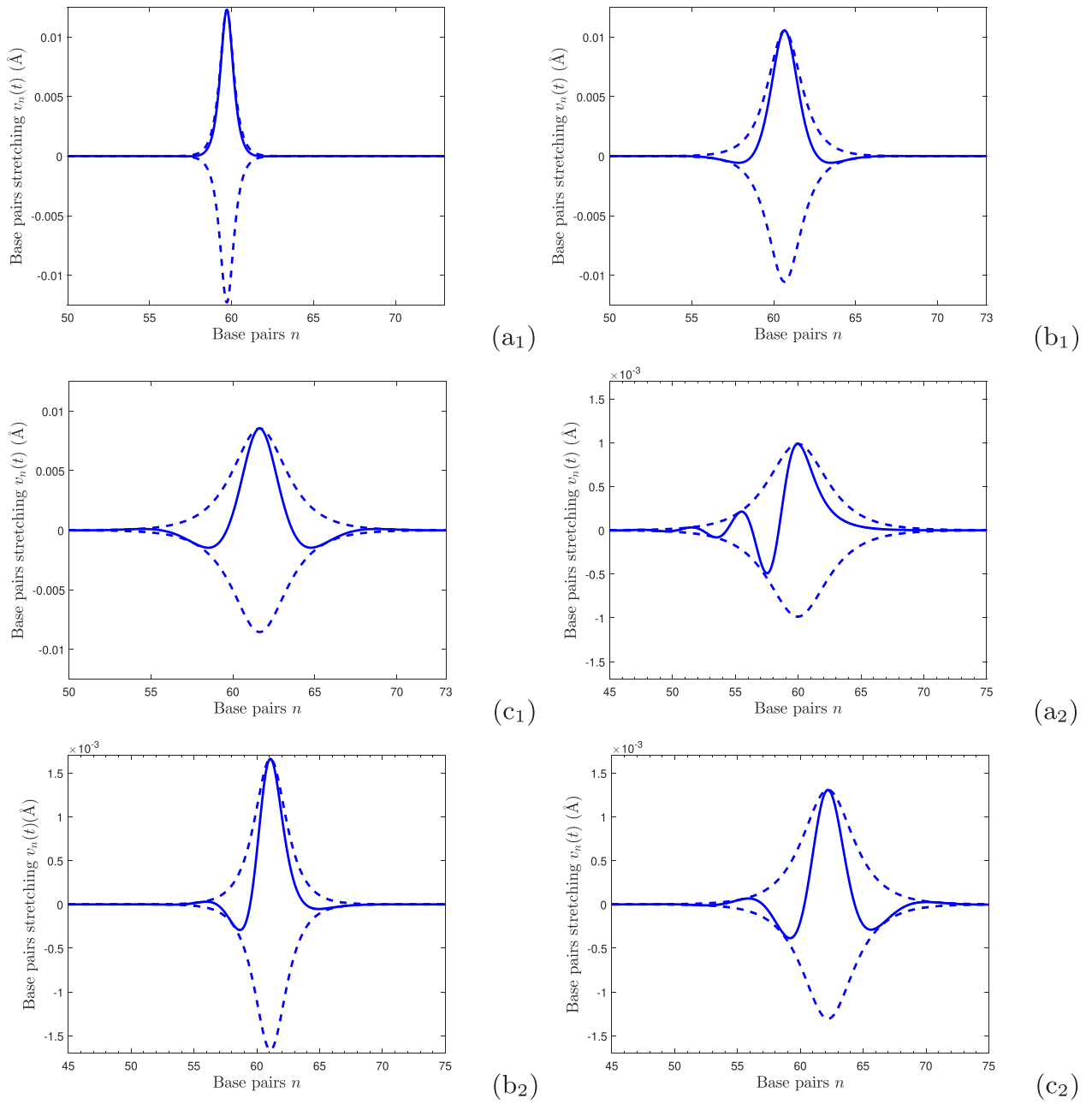

FIG. 11. The stretching nucleotide pairs at $t = 1000$ tu, for three values of the helical interactions constant, namely, $K = 0$ [(a_j), $j = 1, 2$], $K = 0.5K_{\max}$ [(b_j), $j = 1, 2$)] and $K = K_{\max}$ [(c_j), $j = 1, 2$]. Panels (a_1), (b_1), and (c_1) the nonviscous and nonforced medium. Panels (a_2), (b_2), and (c_2) the viscous and forced medium.

and (13) should be equals. Thus, assuming $F_1(x, \tau = \tau_0) = F_{1,\gamma}(x, \tau = \tau_0)$, one obtains

$$f_0 = u_e\sqrt{\frac{1-2\eta}{2P_{2,r}Q_r}}. \tag{38}$$

The final solution $v_n(t)$ of the equation of motion (19) is obtained from Eqs. (20), (21), and (37), in the form

$$v_n(t) = 2F_{1,n}(t)\cos\Theta + 2F_{1,n}^2(t)\left[B_1C_1\cos(2\Theta) - D_1C_1\sin(2\Theta) + \frac{\mu}{2}e^{2\chi t}\right], \tag{39}$$

where

$$F_{1,n}(t) = A_{\gamma,\varepsilon}\,\mathrm{sech}[L_{\gamma,\varepsilon}(nr - v_{g,r}t)],$$
$$A_{\gamma,\varepsilon} = f_{0,\varepsilon}e^{-\Gamma t}, \quad L_{\gamma,\varepsilon} = L_{0,\varepsilon}e^{-\gamma_{1,\varepsilon}t},$$
$$\Omega_{\gamma,\varepsilon} = \omega_r - \varpi_{\gamma,\varepsilon}, \quad \varpi_{\gamma,\varepsilon} = \varpi_{0,\varepsilon} + R_{r,\epsilon},$$
$$\Theta = qnr + \sigma\ln|\mathrm{sech}[L_{\gamma,\varepsilon}(nr - v_{g,r}t)]| - \Omega_{\gamma,\varepsilon}t,$$
$$\Gamma = \gamma_{1,\varepsilon} + \chi, \quad \gamma_{1,\varepsilon} = \gamma_{0,\varepsilon} + R_{i,\epsilon},$$

with

$$f_{0,\varepsilon} = U_e\sqrt{\frac{1-2\eta}{2P_{2,r}Q_r}}, \quad L_{0,\varepsilon} = f_{0,\varepsilon}\sqrt{\frac{Q_r}{2P_{2,r}}},$$

$$R_{r,\epsilon} = \varepsilon^2 R_r, \quad R_{i,\epsilon} = \varepsilon^2 R_r,$$
$$\varpi_{0,\varepsilon} = P_{1,r} L_{0,\varepsilon}^2, \quad \gamma_{0,\varepsilon} = P_{1,i} L_{0,\varepsilon}^2.$$

The real numbers $A_{\gamma,\varepsilon}$, $L_{\gamma,\varepsilon}$, and $\Omega_{\gamma,\varepsilon}$ are, respectively, the amplitude, inverse width, and angular frequency of the soliton solution propagating in the forced-damped medium.

It is well established that the linear gain in the CGL equation usually tends to amplify the noise which eventually perturbs the soliton [84]. However, in the final solution [see Eq. (39)] the effective contributions of the external forces represented by the frequency shift and linear gain are $R_{r,\varepsilon} = \varepsilon^2 R_r$ and $R_{i,\varepsilon} = \varepsilon^2 R_i$, respectively, with $\varepsilon \ll 1$. Thus, the external forces contribution to the whole dynamics is negligible. Hence, the soliton solution found here is stable. As observed above [see Fig. 4(h)], the parameter $\gamma_{1,\varepsilon} > 0$. It behaves like a damping term for the amplitude of the soliton, at the time as a growth terms for its width. Thus, from Eq. (39) one observes that the amplitude and width of the propagating wave strongly depends on time. While the amplitude of the wave decreases exponentially with time following the function $e^{-\Gamma t}$, its width is an exponentially increasing function of time following the function $e^{\gamma_{1,\varepsilon} t}$. The external forces field used here was considered weak, and its contribution to the dynamics negligible as compared to the damping forces. Hence, the amplitude of the resulting dissipative soliton decay, while its width increases as the soliton propagates along the molecular structure. Therefore, the DNA system, as modeled here, loses energy.

The coherency of the soliton solution imposes that the envelope velocity V_e and the carrier velocity V_c, assuming, respectively, as $V_e = v_{g,r}$ and $V_c = \frac{\Omega_\gamma}{q}$, should be equal. Based on this $V_e = V_c$ yields

$$U_e = \sqrt{\frac{4P_{\gamma,r}(\omega_r - q v_{g,r})}{1 - 2\eta}}, \tag{40}$$

with

$$P_{\gamma,r} = \frac{P_{2,r}^2}{P_{1,r}}.$$

From Eq. (39) one obtains the time-dependent expression of the "effective" amplitude $A_{\gamma,m}(t)$ and width $\aleph_\gamma(t)$ of the soliton solution in the damped-forced medium as

$$A_{\gamma,m}(t) = 2A_{\gamma,\varepsilon}\left[1 + A_{\gamma,\varepsilon}\left(\frac{\mu}{2} e^{2\chi t} + B_1 C_1 - D_1 C_1\right)\right],$$
$$\aleph_\gamma(t) = \frac{2\pi}{L_{\gamma,\varepsilon}}, \tag{41}$$

where the amplitude $A_{\gamma,\varepsilon}$ and the width $L_{\gamma,\varepsilon}$ are given in Eq. (39). At the initial times ($t = 0$), we represent, in the panels of Figs. 5 and 6, the evolution of the amplitude $A_{\gamma,m}(t)$ and the width $\aleph_\gamma(t)$ of the soliton in terms of wave number, for different values of the helicoidal coupling parameter K. The plots show that when the helicoidal parameter increases, both parameters increase, decrease, or remain constant depending on the range of variation of the wave number. The same observations can be made in Figs. 7 and 8 in which the amplitude and width have been plotted in terms of K, for different values of the wave number q, at three different instants $t = 0$ tu, $t = 500$ tu, and $t = 1000$ tu. The lines also show the increasing of the width and the decreasing of the amplitude of the soliton with time. For the value of the wave number $q = 0.24$, we notice that the wave is more localized at $t = 0$ when the helical interactions constant is around $K = 1.5.10^{-6}$ eV Å^{-2}; $t = 500$ when the helical interactions constant is around $K = 2.0.10^{-6}$ eV Å^{-2}, and $t = 1000$ when the helical interactions constant is around $K = 2.5.10^{-6}$ eV Å^{-2}. This shows in general that the wave is more localized when the helicoidal interactions parameters takes small values less than the half of the maximum possible value $K \leqslant 0.5K_{\max} = 2.93.10^{-6}$eV Å^{-2}.

C. Numerical investigations

Our aim in this section is to address the behaviors of the DNA open-state configuration represented by the bright-like soliton, when one molecular parameter evolve, namely, the helicoidal constant. We also check the correctness and the stability of our analytical solution (14) [as well as Eq. (13)], and Eq. (39) [as well as Eq. (37)] derived in Sec. III B after some approximations and hypotheses. We also check the long-time evolution and robustness of the analytical solution in the DNA discrete lattice. Therefore, the numerical simulations of the discrete equations of motion (6b) and (19) is done. Our analytical solutions, used as initial conditions, are involved over a very long time with a large lattice. Moreover, we describe a set of numerical experiments using the fourth-order Runge-Kutta scheme with a time step $\Delta t = 10^{-5}$ tu. Our time step is chosen to preserve the total energy of the system to a good accuracy over a complete run. We focus our attention on the width and amplitude of the wave at a given time. The numerical parameters used for simulations are $\eta = 0.47$ and $q = 0.24$.

To start, we use Eqs. (13) and (37) as initials conditions in the first numerical experiment, and we present in Fig. 9 the space-time comparison of the numerical results of the envelope soliton propagating in the nonviscous and nonforced medium [Figs. 9(a) and 9(c)], and viscous and forced medium [Figs. 9(b) and 9(d)]. As predicted analytically, the amplitude and width of the soliton remain uniform during the propagation in the nonviscous and nonforced media. However, by considering the molecule in the viscous and forced environment, the amplitude of the soliton decays in time, at the same time its width increases. Finally the soliton vanishes after a certain time of propagation.

In our second numerical experiment, Eqs. (14) and (39) are used as initial conditions, we compare the spatial evolution of the soliton in the viscous forced, and nonviscous and nonforced medium, at three different instants, $t = 0$ tu, $t = 500$ tu, and $t = 1000$ tu. The results are summarized in Fig. 10, where the respective panels show numerical sketches of the formation of open-state configurations in terms bubble transport in the viscous and nonviscous and nonforced DNA lattice. The solid blue line represents the bubble in nonviscous and nonforced medium, while the dash-dotted red line depicts the bubble in the viscous and forced medium. Figure 10(a) shows a good agreement between both simulations, showing that our analytical solution is robust and suitable to predict the formation of bubbles moving along a heavily damped DNA

chain. The lines also show that the soliton propagates with a constant amplitude and width in the nonviscous and nonforced medium, while taking into account the viscosity and external forces of the medium makes the amplitude to decrease, with a reverse effect on the width. However, as per the analytical predictions, the decreasing of the amplitude is pronounced than the increase in the width.

To see how the helicoidal interactions affect the bubbles dynamics in DNA molecule, in Fig. 11, we depicted our samples as the functions of base pairs position, for three helicoidal interactions constant K, namely, $K = 0$, $K = 0.5K_{\max}$, and $K = K_{\max}$, respectively. Figures 11(a_1), 11(b_1), and 11(c_1) display the bubble propagation in the nonviscous and nonforced medium. As stated in the analytical study (see Fig. 2), one notices the decreasing of the bubble amplitude and increasing of the number of opening base pairs in the bubble, with the helicoidal interactions. In Figs. 11(a_2), 11(b_2), and 11(c_2), we present the bubble propagation in the viscous and forced medium. As predicted by the theory [see dash-dotted green line in Figs. 7(c) and 8(c)], we observe that when the helicoidal interaction constant increases from $K = 0$ to $K = 0.5K_{\max}$, the width of the bubble decreases, while its amplitude increases. However, when the helicoidal interactions constant increases from $K = 0.5K_{\max}$ to $K = K_{\max}$, the width of the bubble increases, while its amplitude decreases.

Finally, one observes that in the nonviscous and nonforced case, the amplitude of the wave decreases linearly, while its width increases linearly as the wave propagates. In the viscous-forced case, the amplitude and width of the propagating wave can increase, decrease, or remain uniform, with changing the helicoidal interaction strength. This is because in the nonviscous and nonforced case, the soliton is conservative soliton, while in the viscous and forced case, base pair oscillations are supported by chirped dissipative soliton for which the dynamics depends also on the viscous-forced character of the systems. Moreover, in both cases, for $q = 0.24$ the angular frequency and group velocity of the wave increase when the helicoidal interaction strength gets pronounced. This implies that the helicoidal force may then affect qualitatively and quantitatively soliton propagation and enhance base pair opening along the DNA homopolymers' lattice.

D. Discussions

As can be seen from Figs. 1 to 8, when the helicoidal interactions increase, the angular frequency, group velocity, amplitude, and width of the soliton can increase, decrease, or remain constant depending on the range of variation of the wave number. These observations also indicate that the impact of helicoidal interactions on DNA dynamics do not depend on its environment. They can be seen as inner DNA mechanisms due to endogenous repair processes within the molecule caused by the actions of some DNA repairs factors, such as *chlorophyllin*.

Although the DNA molecule is naturally inhomogeneous, it contains four different bases with different masses paired in different ways to constitute the genetic code according to a specific sequence such as promotor (P), coding (C), several regulatory regions, (R_1, R_2, R_3), terminator (T). While the G–C pair contains three hydrogen bonds, the A–T pair contains only two hydrogen bonds. Accordingly, the energy interactions for the G–C pair and A–T pair is different. Thus, the base pairs pairing energy in DNA molecule is one-site dependent. Using the quantum-chemical calculations, it was shown that the total energies of stacking (as well as helicoidal) interactions between different types of base pairs depend on the type of interacting base pairs. Indeed, the stacking and helical interactions in DNA systems are not constant, they are functions of the base pairs of interest. So, the change in helicoidal interaction strength has strong biological implications, as it may result from the intrinsic inhomogeneous nature of the molecule.

In nature, it is well known that the external agents present in the DNA crowded environment can attack the molecule more than 10 000 times daily [13], which usually tends to modulate the amplitude, width, and velocity of the propagating bubble, leading to reading or coding errors. What causes genetic mutations and resulting biological pathologies [8–10]. Therefore, changing the helical interactions in DNA systems could be advantageous for the DNA systems since it can reduce or increase the bubble height and width as well as the energy involved by enzymes during the execution of DNA biological processes, what can counteract the harmful actions of external agents and prevent in that sense some coding or reading errors causing genetic mutations and subsequent pathological diseases. The reader should however notice that the case at hand is devoted to an idealized description of DNA, where only DNA and fluid are present. Otherwise, real life is much more complex, which involves temperature fluctuations, inhomogeneities, and many other intrinsic factors that are not included in the proposed model.

The transcription process is well executed with negligible errors when the bubble width is small, while the replication process need a large number of opening base pairs. Since the helicoidal geometry of the DNA molecule can be seen as a natural protection, which contribute to maintain the hydrophobic bases inside the stack, their modification is very important in the biological functioning of the DNA molecule, it modifies qualitatively and quantitatively the dynamics of the molecule.

IV. CONCLUSION

The primary motivation of this work comes from the possibility that some DNA endogenous factors, such as the modification of helical interactions have an impact on the parameters of the open-state configuration moving along the DNA molecule in the form of bubble. The molecule has been taken at the physiological temperature. The helicoidal interactions were added to the original Joyeux-Buyukdagli model of DNA. In the weak external forces field, by considering the molecule in the heavily damped medium, the semi-discrete approximations method was used, taking into account the Stokes and hydrodynamics viscous forces. The dynamics was found governed by a dissipative breather soliton solution of the complex Ginzburg-Landau equation. It came out that the parameters of the open-state configuration, such as the angular frequency, group velocity, amplitude, and width, are functions of the helicoidal interactions. They can increase, decrease, or remain constant when the helicoidal interaction strength evolves, which can counteract the harmful actions of external

agents, which is responsible for unfavorable genetic mutations and resulting biological pathologies. The confirmation of analytical predictions by numerical experiments were done with a good accuracy. In our numerical investigations, we found out that in nonviscous media, the wave travels without vanishing. But, when viscous forces are taking into consideration, the amplitude of the propagating wave progressively decreases, the wave travels for a very short time and vanishes, reducing in the same time the energy involved by enzymes in the execution of DNA biological processes that require the unzipping and opening of the DNA structure.

As the DNA molecule executes its biological functions generally in a noisy crowded environment, we propose to investigate on the quantitative interplay between the external agents and endogenous repairs processes. In an ongoing work, we propose to study the full nonlinear dynamical properties of an inhomogeneous helicoidal DNA chain without considering the external forces as a perturbation.

[1] D. Cai, A. R. Bishop, N. Grønbech-Jensen, and B. A. Malomed, Moving solitons in the damped Ablowitz-Ladik model driven by a standing wave, Phys. Rev. E **50**, R694 (1994).

[2] D. Cai, A. R. Bishop, and N. Grønbech-Jensen, Spatially localized, temporally quasiperiodic, discrete nonlinear excitations, Phys. Rev. E **52**, R5784 (1995).

[3] D. Cai, A. R. Bishop, and N. Grønbech-Jensen, Discrete lattice effects on breathers in a spatially linear potential, Phys. Rev. E **53**, 1202 (1996).

[4] D. Cai, A. R. Bishop, and N. Grønbech-Jensen, Perturbation theories of a discrete integrable nonlinear Schrödinger equation, Phys. Rev. E **53**, 4131 (1996).

[5] A. Mvogo, G. H. Ben-Bolieb, and T. C. Kofané, Discrete energy transport in collagen molecules, Chin. Phys. B **23**, 098701 (2014).

[6] A. Mvogo, J. E. Macías-Díaz, and T. Kofané, Diffusive instabilities in a hyperbolic activator-inhibitor system with superdiffusion, Phys. Rev. E **97**, 032129 (2018).

[7] J. D. Watson and F. H. Crick, Molecular structure of nucleic acids, Nature **171**, 737 (1953).

[8] J. B. Okaly, A. Mvogo, R. L. Woulaché, and T. C. Kofané, Nonlinear dynamics of DNA systems with inhomogeneity effects, Chin. J. Phys. **56**, 2613 (2018).

[9] M. Daniel and V. Vasumathi, Nonlinear molecular excitations in a completely inhomogeneous DNA chain, Phys. Lett. A **372**, 5144 (2008).

[10] M. Daniel and V. Vasumathi, Perturbed soliton excitations in the DNA double helix, Physica D **231**, 10 (2007).

[11] L. Hayflick, How and why we age, Exp. Gerontol. **33**, 639 (1998).

[12] A. Ruiz-Torres and W. Beier, On maximum human life span: interdisciplinary approach about its limits, Adv. Gerontol. **16**, 14 (2005).

[13] A. Klungland and Y.-G. Yang, Endogenous DNA damage and repair enzymes: —A short summary of the scientific achievements of Tomas Lindahl, Nobel Laureate in Chemistry 2015, Genom. Proteom. Bioinf. **14**, 122 (2016).

[14] R. Dashwood and D. Guo, Antimutagenic potency of chlorophyllin in the salmonella assay and its correlation with binding constants of mutagen-inhibitor complexes, Environ. Mol. Mutagen. **22**, 164 (1993).

[15] D. Sarkar, A Sharma, and G Talukder, Chlorophyll and chlorophyllin as modifiers of genotoxic effects, Mutat Res. **318**, 239 (1994).

[16] C. Keshava, R. L. Divi, T. L. Einem, D. L. Richardson, S. L. Leonard, N. Keshava, M. C. Poirier, and A. Weston, Chlorophyllin significantly reduces benzo[a]pyrene-DNA adduct formation and alters cytochrome *P*450 1A1 and 1*B*1 expression and EROD activity in normal human mammary epithelial cells, Environ. Mol. Mutagen **50**, 134 (2009).

[17] J. B. Okaly, A. Mvogo, R. L. Woulaché, and T. C. Kofané, Nonlinear dynamics of damped DNA systems with long-range interactions, Commun. Nonlinear Sci. Numer. Simulat. **55**, 183 (2018).

[18] C. B. Tabi, A. Mohamadou, and T. C. Kofané, Long-range interactions and wave patterns in a DNA model, Eur. Phys. J. E **32**, 327 (2010).

[19] J. B. Okaly, A. Mvogo, R. L. Woulaché, and T. C. Kofané, Semi-discrete breather in a helicoidal DNA double chain-model, Wave Motion **82**, 1 (2018).

[20] J. B. Okaly, F. II Ndzana, R. L. Woulaché, C. B. Tabi, and T. C. Kofané, Base pairs opening and bubble transport in damped DNA dynamics with transport memory effects, Chaos **29**, 093103 (2019).

[21] H. P. Ekobena Fouda, C. B. Tabi, S. Zdravković, and T. C. Kofané, Helicity and wave switching in a nonlinear model of DNA dynamics, J. Phys. Chem. Biophys. **S4**, 001 (2012).

[22] M. Saha and T. C. Kofané, Inhomogeneities and nonlinear dynamics of a helical DNA interacting with a RNA-polymerase, Phys. Scr. **89**, 085003 (2014).

[23] M. Daniel and V. Vasumathi, Solitonlike base pair opening in a helicoidal DNA: An analogy with a helimagnet and a cholesteric liquid crystal, Phys. Rev. E **79**, 012901 (2009).

[24] C. B. Tabi, A. Mohamadou, and T. C. Kofané, Formation of localized structures in the Peyrard-Bishop-Dauxois model, J. Phys.: Condens. Matter **20**, 415104 (2008).

[25] C. B. Tabi, A. Mohamadou, and T. C. Kofané, Discrete instability in the DNA double helix, Chaos **19**, 043101 (2009).

[26] M. Joyeux and S. Buyukdagli, Dynamical model based on finite stacking enthalpies for homogeneous and inhomogeneous DNA thermal denaturation, Phys. Rev. E **72**, 051902 (2005).

[27] S. W. Englander, N. R. Kallenbach, A. J. Heeger, J. A. Krumhansl, and S. Litwin, Nature of the open state in long polynucleotide double helices: Possibility of soliton excitations, Proc. Natl. Acad. Sci. USA **77**, 7222 (1980).

[28] A. C. Scott, A nonlinear Klein-Gordon equation, Am. J. Phys. **37**, 52 (1969).

[29] E. Kengne, A. Lakhssassi, and W. M. Liu, Dynamics of modulated waves in a lossy modified Noguchi electrical transmission line, Phys. Rev. E **91**, 062915 (2015).

[30] G. Gaeta, C. Reiss, M. Peyrard, and T. Dauxois, Simple models of non-linear DNA dynamics, Riv. Nuovo Cimento **17**, 1 (1994).

[31] G. Gaeta, On a model of DNA torsion dynamics, Phys. Lett. A **143**, 227 (1990).

[32] M. Barbi, S. Cocco, M. Peyrard, and S. Ruffo, A twist opening model for DNA, J. Biol. Phys. **24**, 97 (1999).

[33] M. Barbi, S. Cocco, and M. Peyrard, Helicoidal model for DNA opening, Phys. Lett. A **253**, 358 (1999).

[34] U. Dahlborg and A. Rupprecht, Hydration of DNA: A neutron scattering study of oriented NaDNA, Biopolymers **10**, 849 (1971).

[35] G. Corongiu and E. Clementi, Simulations of the solvent structure for macromolecules. I. Solvation of B-DNA double helix at $T = 300$ K, Biopolymers **20**, 551 (1981).

[36] T. Dauxois, Dynamics of breather modes in a nonlinear "helicoidal" model of DNA, Phys. Lett. A **159**, 390 (1991).

[37] M. Peyrard, Nonlinear dynamics and statistical physics of DNA, Nonlinearity **17**, R1 (2004).

[38] J. B. Okaly, F. II Ndzana, R. L. Woulaché, and T. C. Kofané, Solitary wavelike solutions in nonlinear dynamics of damped DNA systems, Eur. Phys. J. Plus **134**, 598 (2019).

[39] M. Remoissenet, Low-amplitude breather and envelope solitons in quasi-one-dimensional physical models, Phys. Rev. B **33**, 2386 (1986).

[40] S. Takeno, Compacton-like modes in model DNA systems and their bearing on biological functioning, Phys. Lett. A **339**, 352 (2005).

[41] T. Moss, *DNA-Protein Interactions*, 2nd ed. (Humana, Totowa, NJ, 2001).

[42] U. Siebenlist, RNA polymerase unwinds an 11-base pair segment of a phage T7 promoter, Nature **279**, 651 (1979).

[43] T. S. Hsieh and J. C. Wang, Physicochemical studies on interactions between DNA and RNA polymerase. Ultraviolet absorption measurements, Nucl. Ac. Res. **5**, 3337 (1978).

[44] S. Zdravković and M. V. Satarić, Parameter selection in a Peyrard-Bishop-Dauxois model for DNA dynamics, Phys. Lett. A **373**, 2739 (2009).

[45] K. Muroya, N. Saitoh, and S. Watanabe, Experiment on lattice soliton by nonlinear LC circuit-Observation of a dark soliton, J. Phys. Soc. Jpn. **51**, 1024 (1982).

[46] B. F. Putnam, L. L. Van Zandt, E. W. Prohofsky, and W. N. Mei, Resonant and localized breathing modes in terminal regions of the DNA double helix, Biophys. J. **35**, 271 (1981).

[47] E. W. Prohofsky, K. C. Lu, L. L. Van Zandt, and B. F. Putnam, Breathing modes and induced resonant melting of the double helix, Phys. Lett. A **70**, 492 (1979).

[48] G. Plopper, *Principles of Cell Biology* (Jones and Bartlett Learning, Burlington, MA, 2012).

[49] A. S. Balajee and M. Phil, *DNA Repair and Human Disease* (Springer Science, New York, 2006).

[50] B. A. Malomed, Bound solitons in a nonlinear optical coupler, Phys. Rev. E **51**, R864 (1995).

[51] G. Cohen, Soliton interaction with an external traveling wave, Phys. Rev. E **61**, 874 (2000).

[52] I. V. Barashenkov and E. V. Zemlyanaya, Travelling solitons in the externally driven nonlinear Schrödinger equation, J. Phys. A **44**, 465211 (2011).

[53] T. S. Raju and P. K. Panigrahi, Optical similaritons in a tapered gradedindex nonlinear-fiber amplifier with an external source, Phys. Rev. A **84**, 033807 (2011).

[54] F. Cooper, A. Khare, N. R. Quintero, F. G. Mertens, and A. Saxena, Forced nonlinear Schrödinger equation with arbitrary nonlinearity, Phys. Rev. E **85**, 046607 (2012).

[55] F. G. Mertens, N. R. Quintero, and A. R. Bishop, Nonlinear Schrödinger solitons oscillate under a constant external force, Phys. Rev. E **87**, 032917 (2013).

[56] N. R. Quintero and A. Sánchez, ac-driven sine-Gordon solitons: dynamics and stability, Eur. Phys. J. B **6**, 133 (1998).

[57] I. Daumont and M. Peyrard, One-dimensional "turbulence" in a discrete lattice, Chaos **13**, 624 (2003).

[58] M. Peyrard and I. Daumont, Statistical properties of one-dimensional "turbulence", Europhys. Lett. **59**, 834 (2002).

[59] J. B. G. Tafo, L. Nana, and T. C. Kofane, Time-delay autosynchronization control of defect turbulence in the cubic-quintic complex Ginzburg-Landau equation, Phys. Rev. E **88**, 032911 (2013).

[60] K. I. Nakamura, H. Matano, D. Hilhorst, and R. Schätzle, Singular limit of a reaction-diffusion equation with a spatially inhomogeneous reaction term, J. Stat. Phys. **95**, 1165 (1999).

[61] C. Sophocleous, Further transformation properties of generalised inhomogeneous nonlinear diffusion equations with variable coefficients, Physica A **345**, 457 (2005).

[62] V. Vasumathi and M. Daniel, Base-pair opening and bubble transport in a DNA double helix induced by a protein molecule in a viscous medium, Phys. Rev. E **80**, 061904 (2009).

[63] J. B. Okaly, A. Mvogo, R. L. Woulaché, and T. C. Kofané, Nonlinear dynamics of long-range diatomic chain, Physica A **541**, 123613 (2020).

[64] A. Sulaiman, F. P. Zenb, H. Alatasc, and L. T. Handoko, Dynamics of DNA breathing in the Peyrard–Bishop model with damping and external force, Physica D **241**, 1640 (2012).

[65] J. Lehmann, S. Kohler, P. Hänggi, and A. Nitzan, Molecular Wires Acting as Coherent Quantum Ratchets, Phys. Rev. Lett. **88**, 228305 (2002).

[66] S. Behnia, S. Fathizadeh, and A. Akhshani, DNA Spintronics: Charge and Spin Dynamics in DNA Wires, J. Phys. Chem. C **120**, 2973 (2016).

[67] A. V. Gorbach, A. S. Kovalev, and O. V. Usatenko, Solitons in a diatomic chain with competing nonlinearities, Phys. Solid State **43**, 2171 (2001).

[68] R. Glaser, in *Biophysics: An Introduction*, 2nd ed. (Springer-Verlag, Berlin, 2012), p. 339.

[69] E. Arévalo, Yu. Gaididei, and F. G. Mertens, Soliton dynamics in damped and forced Boussinesq equations, Eur. Phys. J. B **27**, 63 (2002).

[70] V. L. Ginzburg and L. D. Landau, K teorii sverkhrovodimosti, Zh. Eksp. Teor. Fiz. **20**, 1064 (1950) [Sov. Phys. JETP **20**, 1064 (1950)] [English translation: *On the Theory of Superconductivity*, in L. D. Landau, Collected papers, edited by D. ter Haar (Pergamon Press, Oxford, 1965), p. 546)].

[71] I. S. Aranson and L. Kramer, The world of the complex Ginzburg-Landau equation, Rev. Mod. Phys. **74**, 99 (2002).

[72] L. M. Sieberer, M. Buchhold, and S. Diehl, Keldysh field theory for driven open quantum systems, Rep. Prog. Phys. **79**, 096001 (2016).

[73] I. Carusotto and C. Ciuti, Quantum fluids of light, Rev. Mod. Phys. **85**, 299 (2013).

[74] N. Akhmediev and A. Ankiewicz, *Dissipative Solitons: From Optics to Biology and Medicine*, Lecture Notes in Physics (Springer, Berlin, 2008).

[75] C. B. Tabi, A. Mohamadou, and T. C. Kofané, Modulational instability and pattern formation in DNA dynamics with viscosity, J. Comput. Theor. Nanosci. **5**, 647 (2008).

[76] L. D. Landau, On the theory of phase transitions, Sov. Phys. JETP **7**, 19 (1937); **7**, 627 (1937).

[77] P. Grelu and N. Akhmediev, Dissipative solitons for mode-locked lasers, Nat. Photon. **6**, 84 (2012).

[78] H. G. Purwins, H. U. Bödeker, and Sh. Amiranashvili, Dissipative solitons, Adv. Phys. **59**, 485 (2010).

[79] T. J. Kippenberg, A. L. Gaeta, M. Lipson, and M. L. Gorodetsky, Dissipative kerr solitons in optical microresonators, Science **361**, 567 (2018).

[80] J. Belmonte-Beitia, V. M. Pérez-Garcia, V. Vekslerchik, and V. V. Konotop, Localized Nonlinear Waves in Systems with Time- and Space-Modulated Nonlinearities, Phys. Rev. Lett. **100**, 164102 (2008).

[81] F. II Ndzana and A. Mohamadou, Exact solitary wavelike solutions in a nonlinear microtubule RLC transmission line, Chaos **29**, 013116 (2019).

[82] K. Nozaki and N. Bekki, Exact solutions of the generalized Ginzburg-Landau equation, J. Phys. Soc. Jpn. **53**, 1581 (1984).

[83] N. R. Pereira and L. Stenflo, Nonlinear Schrödinger equation including growth and damping, Phys. Fluids **20**, 1733 (1977).

[84] N. N. Akhmediev, V. V. Afanasjev, and J. M. Soto-Crespo, Singularities and special soliton solutions of the cubic-quintic complex Ginzburg-Landau equation, Phys. Rev. E **53**, 1190 (1996).